Graphical Abstract

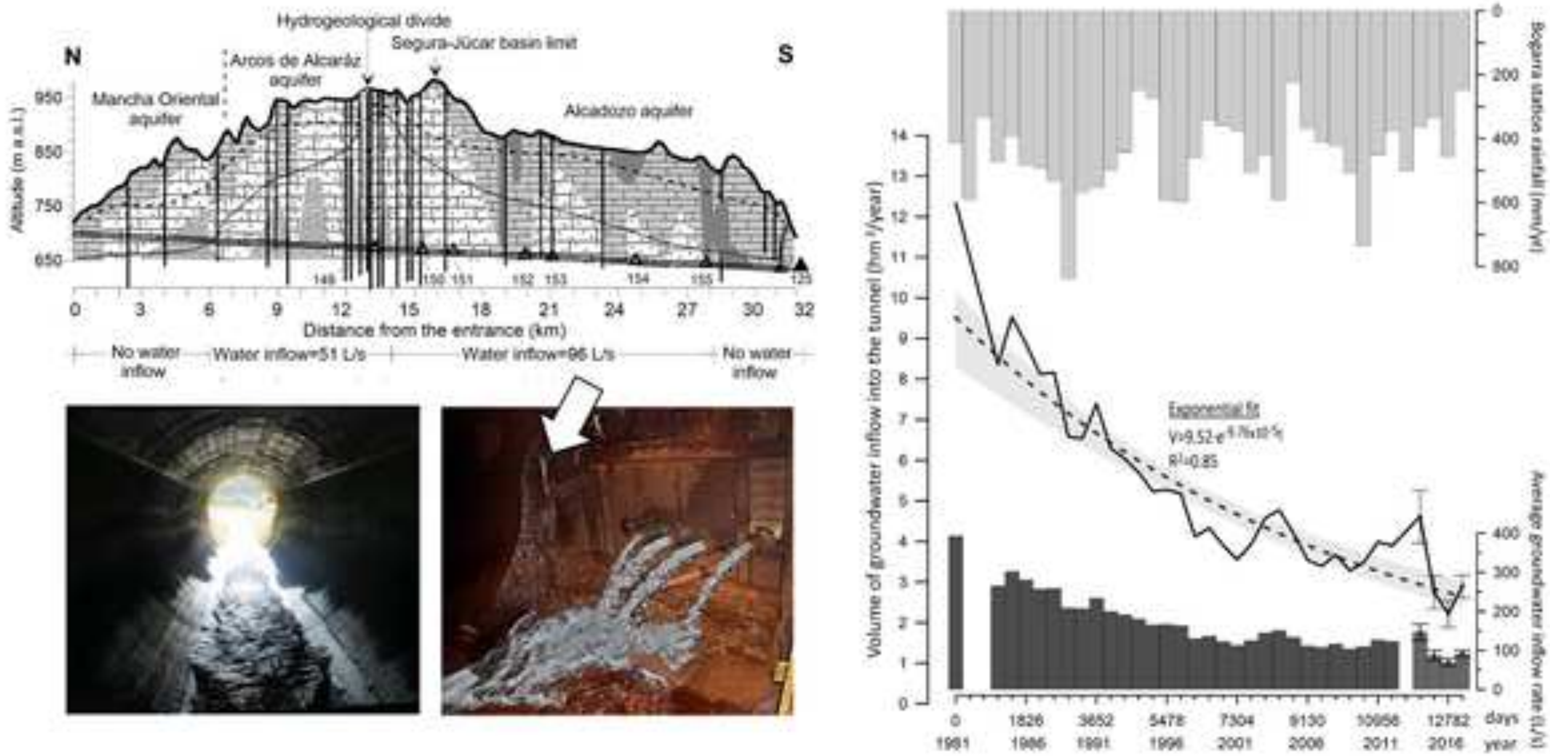

Highlights (for review : 3 to 5 bullet points (maximum 85 characters including spaces per bullet point)

- Between 1969 and 2016, 340 hm^3 of groundwater drained into the Talave tunnel.
- Discharge stabilized in the early 2000's to around 90 L/s.
- All groundwater drained comes from the hydrogeological basin of the Segura river.
- Main groundwater inflows recharge in the Alcadozo aquifer, 20-40 km to the NW.
- Interbasin management must consider not matching surface and groundwater divides.

Deciphering the origin of groundwater inflow into the Talave tunnel (SE Spain)

Jorge Hornero[1]; Marisol Manzano[2], Emilio Custodio[3]

1 Geological and Mining Institute of Spain. Avda. Miguel de Cervantes 45, 30009 Murcia, Spain.

j.hornero@igme.es

2 Department of Mining and Civil Engineering; Technical University of Cartagena. Pº de Alfonso XIII 52, 30203 Cartagena, Spain.

3. Groundwater Hydrology Group, Department of Civil and Environmental Engineering, Technical University of Catalonia. Jordi Girona 1-3, 08034 Barcelona, Spain, Spanish Royal Academy of Sciences

Abstract

The Talave tunnel (TT) is an infrastructure of a major water transfer from the Tajo river basin (center Spain) to the Segura river basin (SE Spain), crossing the Júcar river basin. The tunnel was drilled between 1969 and 1978. It is 32 km long, N/NW-S/SE oriented, has a maximum depth of 320 m, intersects several aquifers, and its southern stretch follows the eastern boundary of the Alcadozo aquifer. The TT drilling perturbed groundwater flow in two river basins, and the induced groundwater inlets generated social and administrative concern lasting until today. The main objectives of this paper are understanding the historical and current tunnel-massif hydrodynamic relationships, and deciphering the origin of groundwater inflow into the tunnel. The first objective was approached analyzing the discharge flow evolution since the drilling until 2016, together with old (1970's) and recent (2014-2017) piezometric data. For the second objective, hydrochemical and isotopic data were generated between 2014 and 2018 from discrete and integrated discharge to the tunnel. Attaining both goals benefited of recent studies on groundwater recharge and functioning in the Alcadozo aquifer. Discharge flows stabilized in the early 2000's. 340 hm^3 were drained between 1969 and 2016, producing a piezometric drawdown between 15 and 120 m along the tunnel. The main inflow zones correspond to tectonic fractures concentrated in the middle and southern sections of the tunnel. The existence of a hydrogeological divide between the Júcar and the Segura river basins some 3 km to the N of the watershed divide implies that all groundwater comes from the Segura hydrogeological basin. The isotopes suggest that groundwater comes mainly from regional flow lines originated to the W of the tunnel, together with some local recharge. The effects of

tunneling can be used to assess the impacts of imminent groundwater development planned by the Basin Authority.

Keywords: Talave tunnel, groundwater level drawdown, groundwater inflows origin, hydrochemistry, water isotopes

1. INTRODUCTION

The knowledge and prediction of groundwater inflow into a tunnel is an important issue in tunnel engineering and drilling, as well as to manage the associated effects on groundwater, springs, wetlands and ecosystems (Chiu and Chia, 2012; Raposo et al., 2010). The spatial and temporal assessment of groundwater inflows into a tunnel is a complex task, not only because of the many geological and hydrodinamic factors governing them (geological structure, hydraulic parameters, hydrostatic pressure, recharge rate, and their spatial and temporal variability), but also due to the often restricted observation conditions. This is especially patent in narrow tunnels for water transport. The possibility of entering these facilities is rare, but direct observation is a priceless opportunity to get information on the interaction between the tunnel and the aquifer.

Most of the works related with the study of tunnel-aquifer interaction have focused primarily on the quantification and prediction of water discharge to the tunnels. These studies have contributed to improve the evaluation of water inflows with sufficient accuracy and using different analytical and numerical methods (Goodman et al., 1965; Perrochet, 2005; Hwang and Lu, 2007; Kolymbas and Wagner, 2007; Park et al., 2008; Gattinoni and Scesi, 2010; Butscher, 2012; Farhadian et al., 2012; Marechal et al., 2014; Su et al., 2017; Li et al., 2018; Farhadian and Nikvar-Hassani, 2019; Xie et al., 2019), most notably include groundwater flow numerical modelling (Perrochet and Dematteis, 2007; Li et al., 2009; Font-Capó et al., 2011; Huang et al., 2013; Hassani et al., 2018; Xiao et al., 2019). Modelling groundwater flow has also been used to study the hydrogeological effects and environmental impacts of excavation-induced groundwater level drawdown (Attanayake and Waterman, 2006; Carrera and Vázquez-Suñé, 2008; Butscher et al., 2011; Chiocchini and Castaldi, 2011; Chiu and Chia, 2012; Jin et al., 2012; Yoo et al., 2012; Vincenzi et al., 2014; Liu et al., 2015; Zhang et al., 2019). The hydrodynamic analysis of aquifers disturbed by tunnelling allows calculating the volume of groundwater discharge to tunnels, taking account the hydraulic conductivity of the massif (Custodio, 2009; Fernández and Moon, 2010; Jiang et al., 2010;

Bagnoli et al., 2015), the recharge to the aquifer (Ofterdinger et al., 2014), the groundwater level (Perelló et al., 2014) and the tectonic and hydromechanical properties of the massif (Zarei et al., 2011; Sharifzadeh et al., 2013).

However, the integrated use of hydrochemical and environmental isotope techniques together with hydrodynamic analysis is scarce in the scientific literature. Most of the available (published) studies using isotopes focus on the origin and/or age of groundwater (Liu et al., 2000; Pastorelli et al., 2001; Marechal, 2012; Liu and Liu, 2015), the hydrological characteristics of the rock formations overlying and around the tunnel (Liu et al., 2005; Moon et al., 2017), the flow regimes (Tomonaga et al., 2017), and the hydraulic connections and the origin of water in mine tunnels (Walton-Day and Poeter, 2009). Yet the join use of hydrochemical, environmental isotope, and hydrodynamic techniques has proved to be very useful to estimating groundwater transit time and discriminating regional/local flow lines (Marechal and Etcheverry, 2003). From the few studies it can be inferred that the use of hydrochemical and isotopic techniques have a great potential to study tunnel-aquifer interactions. The existing applications contributed notably to a better understanding of the role played by both tunnelling and the geological structure on controlling the groundwater flow network in the massif during tunnelling. Nevertheless, their usefulness to explore the long-term influence of tunnel drilling on the regional hydrogeology has not yet been explored. This manuscript considers 40 yr long evolution of groundwater discharge to the Talave tunnel, the current hydrodynamic state and the origin (in a regional aquifer) of groundwater flow lines discharging to the tunnel.

The Tajo-Segura Transfer (TST) transports and distributes water for urban supply and irrigation from the center of Spain (Tajo river basin, in the Atlantic watersheds of the Iberian Peninsula) to the Talave reservoir in the southeast (Segura river basin, in the Mediterranean side of the Iberian Peninsula), through the Júcar river basin. The Talave tunnel (TT) is part of the TST. The excavation of the TT was to overcome a zone of moderate orography located between the Mancha Oriental and Arcos de Alcaráz aquifers, in the Júcar river basin, and the Alcadozo aquifer, in the Segura river basin (Figure 1) (MOP-DGOH-SGOP, 1967). The project considered two aspects that would probably carry problems: the position of the groundwater level above the tunnel, and the presence of faults and discontinuities that could affect the drilling. However the excavation presented much and more significant hydrogeological troubles than forecasted, which caused serious constructive problems that increased the budget and delayed completion due to leaks and structural complexity (MOP-DGOH-SGOP, 1983; García-Yagüe, 1986a, 1986b; Menéndez-Pidal de Navascues, 2006; Pérez-Crespo, 2009). Moreover, the possible drainage of the aquifers traversed and the risk of springs and/or wells drying was a cause of social concern. This controversy persists, in spite of the settlement of legal agreements with the stakeholders after ending the tunnel. Since 1969, -when the TT drilling started- to the present, groundwater inflow takes place in several zones of the tunnel.

This study shows an unpublished part of a comprehensive hydrogeological study of the Alcadozo aquifer (Hornero et al., 2016; Hornero, 2018), in which the information provided by the TT has been used for a better understanding of the regional hydrogeology. A specific research was designed to understand the influence of tunnel drilling on the aquifer hydrodynamics. This research is presented here for the first time. The ultimate objective was to get insight on the long-term impacts of a large work performed in a steady-state aquifer on the regional groundwater levels. Two specific objectives were set to achieve this main goal: (a) understanding the groundwater flow network conditions before drilling the tunnel, their subsequent evolution and the present day tunnel-aquifer relationships, and b) deciphering the source area of groundwater inflows. To attain these aims, the abundant geological and hydrogeological information generated before and during the drilling was collected and analyzed. Furthermore, to get reliable information about the current relationship between the TT and the aquifers, new piezometric, hydrochemical and isotopic data have been generated in the massif around the tunnel, inside it, and at the tunnel outlet. Most of these data were collected and interpreted by the first author in Hornero (2018), and incorporated to the present work together with new information.

2. DESCRIPTION OF THE AREA

2.1. Geology and hydrogeology

The study area is located in the center of the Albacete province, in SE Spain. From the geological point of view, it is part of both the External Prebetic domain of the Betic Range, to the S, and the Tabular Plateau, to the N (Fallot, 1948). The External Prebetic is characterized by a moderate thickness of the Mesozoic cover, formed mainly by Jurassic carbonate rocks (Dogger and Lias) and by the rare presence of Terminal Jurassic (Malm), Lower Cretaceous and Paleogene rocks. This area is characterized by a complex geological structure consisting of a succession of folds and thrusts (Jerez, 1973; Azema et al., 1979; Rodríguez

Estrella, 1979; Baena and Jerez, 1982; Moral, 2005). The main permeable formations are Jurassic limestones and dolomites, which overlay low-permeability Triassic materials (marls, clays and silts with gypsum). The Tabular Plateau consists on detrital Tertiary and Quaternary sediments appearing on a discordant erosional contact over the Jurassic materials.

The TT goes through and interacts with several aquifers, but the most affected is the 454 km^2 Alcadozo aquifer (CHS, 2016; MOP-DGOH-SGOP, 1967) (Figure 1). The legal limits of the Alcadozo aquifer are: to the W, the hydrographic divide between the Guadalquivir and the Segura river basins; to the N, the hydrographic (topographic) divide between the Júcar and Segura river basins; to the S, the course of the Mundo River; to the E, the contact with the Boquerón aquifer, also within the Segura river basin.

Figure 1. Geological map with location of the Talave tunnel (TT), main villages, Mundo river and creeks, Talave dam, aquifers and hydrographic basins in the study area. Also shown are the sampling points inside the tunnel, and the wells, boreholes and springs studied in former works by the authors and whose data area used here as complements.

The climate is semi-arid Mediterranean, except in the highest western sector, where there is a marked continental influence. The relief is rugged (heights range between 1577 m a.s.l. in the W and 944 m a.s.l in the E) and controls strongly the average rainfall (P = 650 to 360 mm/yr, from W to E), and temperature (T = 12 °C in the W to 17 °C in the E). In the eastern part of the study zone, the area crossed by the TT has an average precipitation of 370-400 mm/yr and a temperature of 16-17 °C.

Groundwater hydrodynamics in most of the Alcadozo aquifer is still close to natural conditions. It is mainly controlled by the geological structure and the location of the 2400 km^2 Mundo river basin (Figure 1). The Mundo River is the main drainage axis in this Mediterranean calcareous mountain area, a tributary of the larger Segura river, and is mainly fed by groundwater discharge from Mesozoic carbonate rocks aquifers and from several temporary creeks.

The Alcadozo aquifer is almost unexploited. Local springs and a few wells have been traditionally used to supply small villages. In the last 20 years, irrigated agriculture has grown up in the eastern sector, boosting the drilling of many agricultural wells. Moreover, the 356 km^2 Boquerón aquifer (CHS, 2016) is intensively exploited for agricultural uses, most probably modifying the flow pattern in the eastern part of the Alcadozo system and may be inducing groundwater transfer from this one.

Other aquifers related with the tunnel are the 399 km^2 Arcos de Alcaráz (CHJ, 2016) and the 7118 km^2 Mancha Oriental (CHJ, 2016), both of them in the Júcar river basin (Figure 1). The Jurassic carbonates constitute the main permeable formations. The Mancha Oriental aquifer is more exploited than the other aquifers to supply a higher agricultural demand. The TT crosses both aquifers before reaching the Júcar-Segura basins divide, approximately 15 km to the S of the northern tunnel entrance. From here to the southern entrance, the TT follows the contact between the Alcadozo and Boquerón aquifers along about 17 km. The Mullidar and Heruela creeks (Figure 1), flowing only during intense rainfall events, cross the territory above the Talave tunnel gallery.

Figure S1 shows the main land uses and the agricultural areas. Dominant soils are aridsols-entisols with conifer forests, scrub and some prairies. Crops are mostly rain fed olive trees, vineyards, and winter and spring cereals. In the E and SE parts complementary irrigation and irrigated orchards are proliferating.

In the headwaters of the Segura and Mundo rivers, the Segura river Basin Water Plan for the period 2021-2027 (CHS, 2020) sets up a maximum groundwater exploitation of 10 hm^3/yr. New social irrigation systems supplied with groundwater resources are planned in the study area in order to avoid depopulation, improve local economy, and favor investment in an economically disadvantaged area.

2.2. The Talave tunnel

The TT was drilled between 1969 and 1978 with a length of about 32 km and a diameter of 4.20 m. At that moment, it was the longest water tunnel in Europe. Its altitude is 695.6 m a.s.l. at the northern inlet and 655 m a.s.l. at the southern outlet. The slope is about 0.13 % and water flows by gravity. The thickness of rock above the tunnel exceeds 100 m near the northern entrance and reaches 320 m in its central part.

Drilling was performed by three Robbins tunnel-boring machines. One of the machines was buried at some 13 km from the northern entrance, nearby La Gloria fault (see section 4.1), due to the existence of saturated and little cemented clays, sands and sandstones with a high hydraulic head (Perez Crespo, 2009; Oteo, 2016). This caused months of delay in the excavation. Most of the tunnel was lined with concrete. The complex geological structure and high water pressure motivated the use of reinforced concrete and the placement of drainage pipes in several locations to drain to the tunnel the water accumulated behind the lining. The geological difficulties to overcome can be deduced from the fact that approximately 69 subvertical faults, 3 important overthrusts, and almost 600 m of mylonitic terrain were crossed. A high amount of groundwater stored in the massif was drained to the tunnel during the construction. Groundwater from the different aquifers crossed continued outflowing since then. The Tajo river Basin Authority (CHT) installed and operates since 1984 two automatic gauging systems at the outlet of the tunnel to record the flow rate. This is to quantify how much water is from the TST (transfer) and how much is from groundwater inflow. One of the gauges measures the jointflow (TST plus groundwater inflow) and the other quantifies groundwater inflow when the TST is not operating (Figure S2). Gauging is important administratively to assure that water allocation complies with agreements in the water plans of the Júcar and Segura rivers basins.

3. METHODOLOGY

Several types of data and study methods have been used to achieve the objectives of this work: geological data; old and recent piezometric data; historical discharge flow to the tunnel, and chemical and isotopic data.

3.1. Role of geology and tectonics on groundwater inflow

The detailed geological information generated before and during the construction of the TT by a) MOP-DGOH-SGOP (1983) and b) García Yagüe (1986a) has been analyzed to gain knowledge on the relationships between the permeable formations, tectonics, and the location and relative flow rate of water inflows to the tunnel.

3.2. Groundwater conditions before drilling the tunnel, evolution and present day situation

The groundwater flow patterns before and after tunneling were analyzed. Spatial and temporal water table variations were estimated at regional and local (tunnel) scales. The conditions before drilling were studied using the historical data synthesized in IGME-DGA (2012). To unravel the present conditions, groundwater levels were measured for this research in 22 wells scattered over the entire study area (Figure S3) and in 7 field surveys carried out between 2009 and 2014. Moreover, the altitude of the main springs discharging the Alcadozo aquifer with respect to the Mundo river and the hydrogeological relationship between this stream and the Alcadozo aquifer were analyzed. All the data were used to draw a regional piezometric map representing the present day conditions.

The analysis of the long-term changes of groundwater level in the rock massif above the TT was done by comparing three periods with data: 1968-1973, 1994, and 2009-2014. The data for the period 1968-1973 (observations from 25 piezometers during the construction of the TT) and the summer of 1994 (data from 15 piezometers of a temporal control network operated by the CHT) were provided by the Tajo-Segura Transfer Department of the Tajo river Basin Authority (DTST-CHT). Moreover, 6 of those piezometers were measured for the present research in June 2014, as well as 22 boreholes and wells of the Alcadozo and Boquerón aquifers, in which regional groundwater levels were measured between 2009 and 2014.

3.3. Groundwater discharge to the tunnel

The evolution of groundwater discharge to the tunnel was studied for the period 1981-2017. Flow data were taken from different sources: MOP-DGOH-SGOP (1982b); the CHT gauging systems (period 1984-2012); unpublished data from the DTST-CHT, which conducted a gauging campaign on December 29, 1999 (when the transfer was not operating), in which the main water inflow sites inside the tunnel were located and their flows were quantified; and flow rate measurements performed for this research between 2014 and 2017. The two last set of data allowed evaluating the projections on long-term groundwater inflow made by the CHT in MOP-DGOH-SGOP (1982b).

The information deduced about total discharge since the tunnel drilling was compared with the evolution of regional piezometry and with the average recharge values estimated by Hornero et al. (2016) for the eastern part of the Alcadozo aquifer, where the tunnel is located. In addition, in October 2014, when transfer water in the tunnel ceased, there was a unique opportunity to enter the TT. The authors inside the tunnel performed a differential gauging, in order to quantify the discharge taking place between the Júcar-Segura hydrological divide and the outlet of the tunnel, as well as the inflow from every river basin (considering the coordinates of the different inflow sites and those of the hydrological divide above the tunnel). The flow rate was measured with an impeller flowmeter OTT-FAT Z400 using the conventional velocity–area method (Herschy, 1993). The expression proposed by Sauer and Meyer (1992) was used to calculate the uncertainty of a single discharge measurement.

3.4. Chemical and isotopic characteristics of groundwater discharge and flow lines provenance

In October 2014, groundwater entering the tunnel was sampled for chemical and isotopic analysis (stable isotopes of water and tritium) in 7 drains collecting water from the most important leaking sections (Figure S3) along the TT, and also at the tunnel outlet (integrated flow). The interpretation of the chemical and isotopic data integrated the relationship between the hydrogeological structure of the massif and the tunnel. The thickness of the massif rock, the water column, and the unsaturated zone above the tunnel were compared with the chemical and isotopic values. In addition, the relationship between the isotope values and the chloride (as a natural atmospheric tracer) and NO_3 (as an anthropogenic pollutant) contents were analyzed. A main objective was to identify potential different spatial scales (regional, sub-regional, local) for the source areas of groundwater inflows.

The concentrations of major and some minor and trace solutes were determined by ion chromatography at the Geological and Mining Institute of Spain (IGME). The accuracy of the chemical analyses was obtained from the ion balance error, which was ≤5 % in all cases. Common detection thresholds are about 1 mg/L, with a coefficient of variation of 0.15. The $\delta^{18}O$ and $\delta^{2}H$ deviations from the Vienna Standard Mean Ocean Water (V-SMOW), in delta notation δ (‰, per mil), were measured by mass spectrometry at the CEHIUMA-University of Málaga (Spain). The reported uncertainties were ±0.05 ‰ to ±0.1 ‰ for $\delta^{18}O$ and ±1.0 ‰ for $\delta^{2}H$. The tritium (^{3}H) activity was measured at the Autonomous University of Barcelona by liquid scintillation counting after electrolytic enrichment, with an uncertainty between 0.1 and 0.5 UT, mostly about 0.4 UT.

4. RESULTS AND DISCUSSION

4.1. Role of geology and tectonics on groundwater inflow

A synthesis of the detailed geological cross section generated before and during the construction of the TT is shown in Figure 2, together with flow data measured by the authors in October 2014 inside the tunnel. The excavation found dramatic slide problems related to water inflowing the tunnel in different locations, mainly related with tearing faults and overthrusts in the Middle-Upper Jurassic materials. The main water inflow areas described in those documents are: La Gloria-El Pinar area (some 13 km from the northern entrance to the tunnel), due to the presence of a large mylonitized area with numerous tearing faults and the overthrust of Jurassic saturated carbonates over Cretaceous (Albian) sands, calcarenites and conglomerates; La Reguera area (19-20 km from the entrance), due to the appearance of high permeability Upper Jurassic limestones, and Los Boleros area (25-26 km from the entrance), also due to the existence of Jurassic carbonate materials.

The flow rates measured in October 2014 are consistent with the descriptions of the documents on the drilling progress: between km 6 and 14 (which includes La Gloria-El Pinar area), the measured flow rate of groundwater discharge to the tunnel was 50.65 L/s, and between km 14 and 28 (which includes La Reguera and Los Boleros zones) it was 96.12 L/s. No water inflow was observed outside these two zones.

4.2. Past and present tunnel-aquifer hydrodynamic relationship

4.2.1. Evolution of the groundwater level above the tunnel

The temporal evolution of the groundwater level over the TT since the original conditions to the present is described, according to Figure 2:

- In the first 6 km of tunnel, the initial water column above the tunnel was 20 to 80 m and the groundwater level ranged from 715 to 775 m a.s.l. Data from 1994 to 2017 showed that in this zone and period the water-table was between 650 and 690 m a.s.l. and below the tunnel elevation. This piezometric drawdown could be explained by the significant groundwater pumping for irrigation performed during these decades in wells located at some 10 km to the N and SE of the tunnel, but further information is necessary to check this hypothesis.
- Between km 6 and km 15, the water column above the tunnel was initially between 100 and 240 m, and the groundwater level was up to 890 m a.s.l. and 935 m a.s.l. close to “La Gloria” and “El Pinar” zones, respectively. The large piezometric variation in a quite short distance suggests the existence of a hydrogeological threshold in this zone (Figure 2). This piezometric high coincides spatially with the existence of a tectonic grip of unconsolidated Albian sediments between Jurassic carbonates. The existing data from 1994 and from the period 2009-2014 show the persistence of the threshold. The most recent data allowed estimate the total drawdown produced above the TT in this sector between 15 and 80 m, with the lower values close to the threshold (Figure 2.A).
- From km 15 to km 24 km, the original groundwater levels in the tunnel section were between 825 and 900 m a.s.l. and nowadays they range from 710 to 850 m a.s.l. The total drawdown estimated for the

period 1968/1973-2014 is between 20 and 120 m, but it was much more relevant before 1994 than from this year to the present.

- In the southern sector of the tunnel, from km 24 to about km 32, the groundwater level ranged originally from 735 to 835 m a.s.l. between 1968 and 1973, and currently the water table is located some meters above the tunnel, which is coherent with the regional groundwater flow pattern. The oldest piezometric levels showed some anomalies in the last kilometers as a consequence of the structural complexity around the “Fontanar” “La Heruela” tectonic trench (Figure 2). The coincidence of creeks with faults (Figure 1), the outcrop of the low permeability Triassic materials, and a change of the dominant lithology among the Jurassic series probably induce a compartmentalization of the aquifer at local scale. When all the data are compared, the observed drawdown in this zone was between 35 and 90 m.

The fast water-table drawdown after the construction of the TT was derived from the strong decompression of the aquifer around the tunnel due to the excavation, probably enhanced initially by the increased hydraulic conductivity near the excavation, as has been proposed in other areas (Marechal and Etcheverry, 2003; Li, 2018). After some time, the drawdown tended to stabilize, because of the progressive depletion of the groundwater storage.

Figure 2. (A) Geological cross-section of the Talave tunnel showing the inferred groundwater level changes caused by its construction, critical hydrogeological zones along the tunnel, location of the main water inflow sites, sampling sites in October 2014, and groundwater inflow rates measured in the same date. The initial groundwater level represents the situation in 1968, and the present-day groundwater level represents the situation since 2014. (B) Major faults crossed by the tunnel. See location in Figure 1.

4.2.2. Temporal evolution of groundwater discharge

Figure 3 shows the water inflows to the tunnel, after DTST-CHT on its survey of December 29, 1999. The distribution of the preferential drainage sections along the tunnel seem to stay the same over time in the period 1980/81 to December 1999. Water inflow is produced along almost the entire tunnel. Individual flows are commonly <2-3 L/s. The added highest inflows measured in December 1999, between 17 L/s and 53 L/s, were identified in “La Gloria”, “El Pinar” and “La Reguera-Pozo 5” areas (see Figure 2).

Considering their location in the tunnel and the position of the Júcar-Segura hydrological divide, the inflows from the Júcar and Segura river basins would be 69 L/s and 52 L/s, respectively, at the moment of the survey. Moreover, taking into account the data provided in MOP-DGOH-SGOP (1982b), the water inflows in "La Gloria" area decreased from about 200 L/s to 50 L/s between 1981 and 1999. In the other areas, the inflows registered in 1999 were close to stabilization.

Figure 3. Evolution of total water inflow along the Talave tunnel in December 29, 1999, and location of the main inflows at a point or short length. Distance from the entrance at Los Anguijes.

The time series of groundwater inflow in the tunnel are shown in Figure 4, with precipitation data at the Bogarra station. The measured annual groundwater inflow volumes and estimated average inflow rates for the period 1981-2012 are shown in Table 1, and the measured water inflow and estimated volumes for the period 2014-2017 are shown in Table 2. There is a good exponential fit (R^2=0.86) for the recession curve (Figure 4), with an estimated average recession coefficient for the whole observation period α_{TT} = $9.76 \cdot 10^{-5}$ d^{-1}. Considering the dimensions of the Jurassic aquifer on a regional scale, this α value is consistent with the ones provided by MOP-DGOH-SGOP (1982a) for influence radius between 6000 and 10,000 m, with a storage coefficient value for the unconfined aquifer $S=10^{-2}$, constant transmissivity, and assuming steady state conditions.

Table 1. Annual water inflow volume to the Talave tunnel for the period 1981-2012, measured at the southern output. Source: DTST-CHT.

Table 2. Gauged flow rates at the exit of the Talave tunnel in different dates and estimated yearly volumes. Also shown is the flow rate measured on 29/10/2014 inside the tunnel, just in the Segura-Júcar basins divide. Source: own data.

The average α_{TT} value is two orders of magnitude smaller than the estimated by Hornero et al. (2016) for large springs in the area ($\alpha_S = 3.5 \cdot 10^{-3}$ d^{-1}), but it is consistent with the different spatial scales of the massif volumes involved and with the heterogeneity of the rock massif. This agrees especially with the expected variability of the permeability with depth in the active massif thickness, in the same way that Tsang and Niemi (2013) suggested in a study on deep aquifers. The α_{TT} is a measure of the regulation capacity of a large aquifer volume, which in this case corresponds to a groundwater dynamic storage above the tunnel of >1000 hm^3, in coherence with IGME-CHS (2009). The α_S corresponds to the regulation capacity of smaller aquifer volumes feeding the Alcadozo springs.

The water inflow to the TT decreased from 12.30 hm^3/yr (390 L/s) to 2.89 hm^3/yr (90 L/s) between 1981 and 2017. The average flow rate for the whole study period is approximately 170 L/s. Considering the evolution of annual inflows in Figure 4, and taking into account the uncertainty, it is reasonable to assume that in recent years (2015, 2016 and 2017) the flows approach minimum values. Stabilization seems to have occurred around year 2001, with a volume of about 3.6 hm^3/yr. The fact that piezometric levels have remained without significant changes in recent years is consistent with the steady state conditions of the Alcadozo aquifer and with the stabilization hypothesis of groundwater discharge to the TT.

The correlation between annual precipitation and average flow rate is very poor (R^2=0.04), but the inflow function shows some peaks in years 1985, 2001, 2004 and 2013 which seem influenced by high temporal precipitation, with seasonal influence. This is expected in semiarid areas (Scanlon et al., 2006; RAEMIA, 2019; Sophocleous, 1992). In the semiarid area of the Alcadozo aquifer, recharge is mostly produced by the precipitation of the first half of the hydrologic year (October to April) (Hornero et al., 2016), and average recharge is spatially variable. For example, recharge in the catchments of the Ayna and Liétor main springs (see Figure 1) is 35 to 50 mm/yr, with a coefficient of variation of 0.35 to 0.50. In some areas of the aquifer recharge may exceed 200 mm/yr. Average recharge is 0.06 to 0.10 of average rainfall, although poorly correlated (Hornero, 2018), as commonly happens under semiarid conditions (RAEMIA, 2019).

Figure 4. Annual evolution of the total groundwater inflow to the Talave tunnel in the period 1981-2016 (hm^3/year), exponential fit and confidence range. The average water inflow rate (in L/s) and the annual rainfall (mm/yr) in the reference station (Bogarra) are also indicated. Source: elaborated from data provided by the Technical Head of the Tajo Basin Water Authority (total inflow drained and average inflow), Spanish Agency of Meteorology (pluviometry), and own data (total drainage at the tunnel exit and average inflow for the period 2014-2016, with the estimated ±2σ uncertainty strip).

To quantify the water table lowering due to the drilling of the tunnel, the current regional piezometry was compared with the inferred values before tunnel construction (Figure 5). The water table decreased between 60 and 100 m around the central sector of the Alcadozo aquifer. The information collected from various sources, adding the data generated for this study, allowed quantifying to about 340 hm^3 the total volume of groundwater drained into the tunnel during the period 1969-2016.

Under steady state flow conditions, the aquifer-tunnel equilibrium implies that the drainage (Q) after a certain time (t) is similar to the average recharge ($\bar{R}$) to the aquifer in the influence area [Q → $\bar{R}$ for t >> 0]. Thus, considering the recharge area in the Alcadozo sector (≈150 km^2) and a total water inflow to the tunnel of 318 hm^3 in the period 1969-2007, the estimated piezometric lowering varies between 69 and 104 m for porosities of 0.02 and 0.03, respectively. Considering the hydrogeological heterogeneity, this estimation agrees with the significant subregional piezometric drawdown inferred from historical piezometries. The piezometric lowering calculated by groundwater flow numerical modelling (Hornero, 2018) is quite similar for a large part of the aquifer (70-130 m), although the location of some limits and the boundary conditions are uncertain.

4.2.3. Influence of tunnel drilling on regional piezometry

Figure 5.A shows the regional piezometry and groundwater flow pattern before drilling the TT. The regional groundwater flow pattern showed a preferential circulation from the NW toward the S, SE and E limits of the Alcadozo aquifer. Thus, groundwater recharged in the northern part of the aquifer was transferred to the main discharge areas in the S and SE. Existing uncertainties about the location of the eastern limit (Hornero, 2018) allows considering a groundwater transfer to the Boquerón aquifer.

During the field works of this study (2009-2014), some piezometric measures were acquired in new wells located in the vicinity of the TT. Figure 5.B shows the regional piezometry of this period. The main regional groundwater flow is also from NW to SE. Most groundwater discharge takes place through two large spring areas located in Ayna and Liétor villages, to the S and SE, near the Mundo River. Some discharge also occurs as diffuse flow to the Mundo river along the aquifer southern border (IGME-CHS, 2009; Ortega et al., 2015). However, the regional flow scheme already shows influence of the TT and of the agricultural groundwater exploitation in the eastern sector of the Alcadozo aquifer and in the nearby Boquerón aquifer. This scheme allows knowing the current hydrodynamic situation: the main regional features of groundwater flow are maintained, but there is a clear influence of drainage to the tunnel and of groundwater exploitation for irrigation. The groundwater transfer between contiguous aquifers has not been wiped out by the drainage to the tunnel.

The current piezometry highlights the persistence of a hydrogeological threshold close to km 13 from the northern entrance of the tunnel. This divide is located to the N of the Segura-Júcar rivers basins hydrographic divide. As discussed in section 4.2, it seems that tunneling favored groundwater inflow through faults, with the subsequent fast drainage of the less consolidated, saturated formations (Albian calcarenites and sands/clays) (Oteo, 2016), which are tectonically clamped between Jurassic carbonates. It is a complex tectonic contact with hydrogeological implications that would explain local effects on permeability distribution and groundwater levels.

Figure 5. Regional piezometry of the study area in different times. (A) Natural regime in the Alcadozo aquifer before drilling the tunnel (modified from IGME-DGA, 2012). (B) Period 2009-2014, with piezometric data from the Alcadozo aquifer and from the Talave tunnel (own data). The measurement points are shown.

4.3. Origin of groundwater inflows to the tunnel

4.3.1. Information provided by hydrochemistry

The concentration of major ions, main physic-chemical characteristics, and isotopic values of the groundwater inflow samples taken in October 2014 inside the tunnel (samples 149 to 155) and total flow at the southern tunnel exit at different dates (samples 125a,b,c,d,e) are shown in Table 3. In general, waters are of the CaMg-HCO_3 and MgCa-HCO_3 types and similar to groundwater in the Alcadozo aquifer, in coherence with the main lithology. Data are shown in figures S4 and 6.

Table 3. Physico-chemical values and isotopic contents of the water inflows sampled inside the tunnel (149 to 155) and of total flow at the outlet (125).

Local groundwater chemical composition is the result of the following common processes:

a.- Atmospheric deposition of salts originated in the sea, contained in dust from far away continental sources and locally recirculated. Chemical analyses of rainfall in several locations of the Alcadozo aquifer can be found in Hornero (2018). Local circumstances favor a dominant origin of Cl and Na from the sea. The most frequent values are 0.6 ± 0.3 $g/m^2/yr$ after Hornero (2018) or slightly higher after Alcalá and

Custodio (2008a, 2008b), with a coefficient of variation of 0.3 (Alcalá and Custodio, 2004; 2012; 2015). SO_4 is partly of marine origin and partly from continental sources related to fossil fuel combustion, among them a relatively close coal power plant. The marine ratio $rSO_4/rCl = 0.12$ (r = concentration in meq/L) may increase up to more than 2, depending on dominant winds.

b.- Dissolution of local rocks. The TT goes mainly through carbonates (Jurassic), but due to the intense tectonic deformation of the area it also crosses clays and silts with gypsum (flakes of Triassic Keuper) and siliceous sands (Cretaceous Albian). Moreover, part of the tunnel layout is covered by carbonated sands (Miocene and Quaternary). The dissolution of carbonates, induced by the dissolution of soil CO_2 at moderate partial pressure (vegetation under semiarid conditions) contributes Ca^{2+}, Mg^{2+} and HCO_3^-, which dominate groundwater chemical composition. The dissolution of gypsum contributes Ca^{2+} and SO_4^{2+}.

c.- Evapoconcentration of soil water through evaporation and transpiration, which increases ion concentration up to saturation in calcite and dolomite, but the solution is clearly undersaturated relative to gypsum. The water excess is in-transit recharge that moves to the saturated zone. Saturation limits the Ca^{2+}, Mg^{2+} and HCO_3^- contents. No large chemical changes are expected during percolation and later flow in the saturated zone, except minor precipitation-dissolution sequences that may affect the Mg/Ca ratio.

d.- Other contributions of soluble salts, in this case mostly fertilizers in the cultivated areas. There are no data on this contribution, which is probably highly variable spatially and different in the dry farming areas relative to the irrigated ones. Most of the western side cultivated areas are rain fed and applied fertilizers are probably manure and ammonium sulphate. If this were the case, the whole SO_4^{2+} would incorporate to groundwater, as well as the non-consumed part of nitrogen, directly as NO_3^- or indirectly after oxidation in the atmosphere of volatilized NH_3.

The chemical composition of the sampled inflows shows a general decrease of electrical conductivity (EC) and ions concentration from N to S (Figure 6), although some changes are close to the analytical uncertainty. Sulphate shows the largest changes. Though Ca^{2+} evolution reflects mainly that of HCO_3^-, some samples (i.e. sample 153) show a correlation between Ca^{2+} and SO_4^{2+}, reflecting mostly the influence of gypsum dissolution from the flakes of Triassic Keuper cut by the tunnel. Thus, part of the SO_4^{2+} can be from fertilizers, but the contribution of gypsum must be considered.

Figure 6. (A) Evolution of major ion concentrations, electrical conductivity (EC), pH, and Cl/Br molar ratio values in seven individual groundwater inflows taken in October 2014 along the Talave tunnel (samples 149 to 155) and in sample 125 of total flow taken at the southern exit of the tunnel, as well as in site 125 in October 2012, April 2015, February 2016 and October 2016. (B) Schoeller-Berkaloff diagram of the chemical composition of the same samples. Modified from Hornero (2018).

The relatively high concentrations of NO_3^- in all the samples (18-39 mg/L) can be explained by recent irrigation return flows from agriculture all along the layout of the tunnel, which is more intense in the central sector and towards the E. A sharp increase of NO_3^- in sample 154 points to local recharge at the southern sector of the tunnel, which is consistent with the regional hydrodynamic disconnection hypothesis that has been proposed before for this section of the tunnel. The NO_3^- content in springs away from irrigated areas is low and even close to zero.

The Cl/B molar ratio tend to decrease down flow, which should not happen if the origin of the anions is marine (Cl/Br = 655), assuming the changes are less than the uncertainty. According with Alcalá and Custodio (2008b) and Custodio and Herrera (2000), the decrease could be explained in this case as the effect of application of Br^- containing herbicides and fertilizers in the eastern and southeastern irrigated areas.

The pH tends to increase down flow, which may reflect a greater contribution of return irrigation flows. The lower mineralization of samples 154 and 155 coincides with the greater groundwater inflow observed in this part of the tunnel. Thus, water inflow from local recharge seems to be a main feature in the southern sector of the TT. However, the concentrations measured in the total outflow at the exit of the tunnel in site 125 reflect a larger relative contribution of inflows from the northern sector of the tunnel.

In synthesis, there is a general down flow decrease of groundwater mineralization and the shape of the flow lines suggests different origins and residence times in the massif along the tunnel. Most likely, the combination of the type of porosity (primary in shallow detrital formations and secondary in deeper Jurassic carbonate formations) with the existence and location of fractures plays a relevant role in the flow net pattern in the massif (Hornero, 2018).

The study of bivariate relationships provides an insight on the sources of solutes and of groundwater. In general, SO_4^{2-} is not correlated with NO_3^-, supporting the hypothesis of a main lithologic origin (Figure S5.A). This is consistent with the location of the samples with highest SO_4^{2-} contents in the central sector of the TT, where almost 100 m of Triassic formations were crossed (Menéndez-Pidal, 2006).

There is a positive covariance of NO_3^- and Cl^- in almost all the water samples, except in sample 154 (Figure S5.B). This points to the relevance of evaporation of return irrigation water, as the only significant source of Cl^- in groundwater is expected to be atmospheric deposition. The average Cl^- concentration in rainwater is 1.8 mg/L in the nearby Bogarra station (Hornero, 2018), which is equivalent to a deposition of 0.7 g/m^2/yr. Considering the Cl^- concentration in groundwater, the evapoconcentration factor is around 5-7 times. Its inverse value agrees with the average recharge to rainfall ratio. The positive correlation of NO_3^- and the Cl/Br ratio in most samples (Figure S5.C) also supports the evapoconcentration hypothesis. Exceptions suggest that groundwater follows different flow paths and is a mixing of waters from various recharge areas.

In spite of the chemical variability of the different groundwater inflows to the tunnel, two groups with different mineralization, but similar chemical composition, have been identified, which suggests two main origins for the water samples. The most mineralized water inflow group is found in the central sector of the tunnel (samples 149, 150, 151, 152 and 153, with EC around 600 µS/cm), and the least mineralized group is found in the southern sector (samples 154 and 155, with EC around 425 µS/cm). A mixing line between two end-members describe the composition of the total water outflow at the tunnel exit (sample 125), which is a weighted mixture of both groups of water inflows to the tunnel (Figure 7). Samples 125a-to-d can be explained as binary mixtures of the end-members (Figure 7), with deviations explainable by precipitation of calcite and dilution of groundwater in the S sector by local enhanced recharge.

Figure 7. Concentrations of some major solutes (HCO_3^-, Ca^{2+}, Cl^- and Na^+, in meq/L) versus EC (µS/cm) in water sampled inside the tunnel in October 2014 (149 to 155) and at the tunnel exit in different years (125a to e). The figures show the existence of two main chemical groups contributing water to the tunnel, one in the central sector and another in the southern sector. The deviations may be explained by calcite precipitation and additional return irrigation flows.

The total groundwater composition in the tunnel outlet, in samples 125a,b,c,d,e (Table 3) does not show significant temporal variations. The small decrease of EC and ion concentrations in samples 125a,c,d,e (October 2012, April 2015, February and October 2016) relative to sample 125b (October 2014) can be the result of recharge episodes before the sampling surveys. Therefore, the hydrochemical characteristics of sample 125b can be considered representative of the current relationship between the tunnel and the groundwater flow around it.

4.3.2. Information provided by water isotopes

The water isotopic contents of $\delta^{18}O$ and $\delta^{2}H$, the deuterium excess value (d), and the tritium activities (^{3}H) of water inflow samples are shown in Table 3. The stable isotope composition varies from -6.3 ‰ to -8.1 ‰ for $\delta^{18}O$ and from -45 ‰ to -54 ‰ for $\delta^{2}H$. This suggests recharge at different heights, once the slope effect is compensated (Custodio and Jódar, 2016) to take into account that the isotopically depleted recharge produced up flow dilutes down flow groundwater recharge when sampling large springs or deep pumped wells.

Figure S6.A shows a plot of isotope data of the groundwater inflow samples and the Global Meteoric Water Line (GMWL) with d = +10 ‰ (Craig, 1961) and the Western Mediterranean Meteoric Water Line (WMWL) with d = +13 ‰ to +14 ‰ (Araguás-Araguás, 1991; Jiménez-Martínez and Custodio, 2008). The water samples plot close to the GMWL and precipitation of Atlantic origin (Plata, 1994) generated at different altitudes. Some deviations are possibly due to evaporation under semiarid conditions during rainfall and in the upper soil before generating recharge. The large deviation of sample 154, the isotopically heaviest one, is a common situation under these circumstances. Samples 154 and 155, the heaviest ones, point to recharge at a lower altitude than for the other groundwater points.

Figure S6.B shows the $\delta^{18}O$ altitudinal isotopic gradient estimated by Hornero (2018) from rainfall and spring data in the Alcadozo aquifer. The apparent $\delta^{18}O$ gradient is about -0.45 ‰/100 m, which is within the range from -0.15 to -0.50 ‰/100 m estimated for rainfall by Clark and Fritz (1997) and close to the average -0.35 ‰/100 m estimated for Spain by REVIP/AEMET/CEDEX (http://www.cedex.es). The highest absolute values represent better the rainfall altitudinal gradient (RAEMIA, 2019), except where strong vertical airflows are produced. If the possible evaporative enrichment is taken into account, samples 149 to 153 were recharged probably between 1300 and 1400 m a.s.l. These heights are not consistent with the altitudes along and nearby the tunnel, which vary between 700 and 950 m a.s.l. However, the range of heights for samples 149 to 153 is consistent with the altitudes existing in the northern recharge area of the Alcadozo aquifer, some 30-40 km to the NW of the tunnel, and the heights deduced for samples 154 and 155 are consistent with the altitudes existing some 20 km to the NW of the tunnel (Figure S7). The altitudes to the E of the tunnel are lower than 1000 m a.s.l. Thus, the recharge areas deduced with stable isotopes suggest the predominance of regional flows for samples 149 to 153 and subregional flows for samples 154 and 155.

In the first half of the 2010 decade, all water samples contained measurable ^3H, between 0.2 ± 0.1 and 2.3 ± 0.2 TU. These values are consistent with those measured in a large number of groundwater samples taken from wells and springs, across the whole Alcadozo aquifer system in 2012 and 2013, which varied between 0.6 ± 0.5 and 5.4 ± 0.6 TU (Hornero, 2018). The ^3H values measured in rainwater between 2000 and 2016 in nearby stations of the REVIP/AEMET/CEDEX network (Murcia, Ciudad Real and Madrid; http://www.cedex.es) range from 1.5 to 10 TU. The most common values measured in Ciudad Real (some 150 km to the NW of the study area), which is the closest station and has similar atmospheric conditions to the study area, are between 3.95 and 6.12 TU. These values indicate that, at least since the year 2000, the average tritium content in rainwater is currently approaching the natural value, as claimed by Castaño and Rodríguez-Arévalo (2019). However, by the mid-1990s, rainfall on the Iberian Peninsula still had some thermonuclear ^3H and its contents were around 7-10 TU (Plata, 2006).

The quantitative interpretation of ^3H data needs a reliable conceptual flow and mixing model, but available data is too scarce. Mass transport with recharge in the porous and moderate karstified unsaturated medium may be delayed from months in the karstified parts to several decades in the sedimentary materials, with possible high dispersion. Regional groundwater flow can be described by an exponential mixing model recharged over the full area, especially for the Alcadozo aquifer sector to the W and NW of the tunnel. After the probable saturated thickness, drainage porosity and recharge at intermediate scale, the renewal time can be estimated to be of several decades, yielding a tritium concentration of a few tenths of TU at the outflows. This approaches what is observed, although large spatial variations can be produced due to the different penetrations of the sampling points and the heterogeneities.

According to stable isotopes, most waters with <0.6 TU, and sample 149, in the central sector of the tunnel, should come from the area placed 30-40 km to the W and NW. Samples 154 and 155 have low tritium content, low EC (430 µS/cm) and medium to high NO_3^- content (39 and 14 mg/L). They should come from some 20 km to the NW (Figure S7). High NO_3^- and low EC suggest excess irrigation flows applying low mineralized irrigation water, and low tritium contents means long residence times. A hypothetic explanation is that these two samples are mixtures of sub-regional flow lines from the carbonate massif to the NW (Figure 1 and Figure 5.C) and local rainwater infiltrated in the porous sediments of the Mullidar and Heruela sporadic creeks, whose layout follows main faults (Figure 1), leaching NO_3^- from the agricultural soils in their basins.

Samples 150, 151, 152, and 153, from the central sector of the tunnel, have tritium concentrations between 0.7 and 2.5 TU (Table 3). According to the stable isotope content, they should come from the highest recharge area in the Alcadozo aquifer, some 30-40 km to the NW of the tunnel. High EC values (Figure 8. A-C) and relatively high and covariant NO_3^- and Cl^- values (Figure S5.B) show the presence of excess irrigation water, which points to a closer water source. The composition of these samples can be explained as mixtures of regional groundwater flow lines reaching the western part of the tunnel, with recharge of excess irrigation water over the central and northern part of the tunnel, where irrigation is performed with groundwater from wells tapping also regional flow lines. No correlation between ^3H and EC and NO_3^- may be expected (Figure 8.A-B), as the involved processes are different, but there is some correlation between $\delta^{18}O$ and EC as their values result from the same processes. Sample 149 has a similar isotopic composition to the former set, but its relatively high EC (610 µS/cm), NO_3^- (31 mg/L) and Cl^- (26.8 mg/L) values and low ^3H content (0.4 ± 0.2 TU) points to a larger contribution of excess irrigation water.

Figure 8. Tritium activity in the water inflow samples taken inside the tunnel (149 to 155) and in total water outflow at the tunnel exit (125) versus (A): Laboratory EC; (B): NO_3^- concentration. It can be observed that the water inflows mainly contributing to the total water outflow from the tunnel are 155 and 151 (circled area), while the contribution of the others (dotted area) is negligible compared to these last ones; (C) $\delta^{18}O$ values measured in the water inflow

samples taken inside the tunnel (149 to 155) and in the total water outflow at the tunnel exit (125a to e) versus EC values. Sample 151 has been used as representative of the tunnel central sector end-member.

From Figure 8.A-B it can also be inferred than groundwater inflows 151 and 155 contribute mainly to total flow into the tunnel. This is confirmed by the relationship between $\delta^{18}O$ and EC (Figure 8.C). Based on the information provided by Figure 8, an estimation of the relative water input to the tunnel through the central and southern sections has been performed by isotopic mass balance. Sample 125 has been considered a binary mixture of two end-member waters represented by samples 155 and 151. As mixing proportions are quantified using conservative components (in the short term when tritium is included) that are part of the water molecule, the proportions are equivalent to flow proportions. The mass balance equation is:

$$(\delta, {}^{3}H)\ \text{Mix} = x\ (\delta, {}^{3}H)\ \text{Central sector inflow} + (1-x)\ (\delta, {}^{3}H)\ \text{Southern sector inflow}$$

where δ are the stable isotope contents and ^{3}H tritium activity; x is the proportion of central sector water inflow in the mix, and 1-x is the proportion of southern sector water inflow.

Table 4 shows the mixing proportions calculated from the October 2014 samples. Tritium and $\delta^{2}H$ yield similar proportions. The results roughly indicate that around 75 % of the total flow in the tunnel would come from the central sector and the remaining 25 % from the southern sector. Considering the geographical position of the rivers basins divide and of the inflow 151 (located in the northern limit of the Alcadozo aquifer, which is also the river basin limit, Figure 14), this could imply that most of the flow is recharged in the Segura river basin, though sample/inflow 151 seems located just on the divide. Taking into account the uncertainties, this is consistent with the results of differential gauging conducted in October 2014 within the tunnel: about 35 % of the flow was recharged in the Júcar river basin and the remaining 65 % in the Segura basin. However, the existence of a groundwater divide some km to the N of the hydrographic divide (see Figure 2) means that the total inflow to the tunnel would be drained from the groundwater part of the Segura basin.

Table 4. Estimated relative contribution of the main water inflows from the central and southern sectors of the tunnel to the total water outflow (sample 125) in October 2014.

5. CONCLUSIONS

The integrated analysis of geological, hydrogeological, hydrochemical and isotope data with diverse study tools, allowed obtaining unprecedented knowledge on the past and present relationship between the Talave 32 km long tunnel, drilled in the 1970s, and the Alcadozo aquifer, and on the present day sources of groundwater discharging into the tunnel.

The geological information generated before and during the construction of the TT allowed insight on the relationship between the permeable formations and the tunnel, and the main role of tectonics. Water inflowing the tunnel was mainly related with overthrusts of Middle-Upper Jurassic materials. Moreover, the primary reason inducing increased groundwater inflows during the drilling was tectonic, as the larger inflows appeared in zones of large faults or intense fracturing. In addition, a tectonic grip of less permeable Albian (Cretaceous) sands, conglomerates and clays between very permeable Jurassic marls and limestones, which is located almost in the middle of the tunnel (km 13-14), produces a hydrogeological threshold that originates a groundwater divide between the Júcar (to the N) and the Segura (to the S) basins.

The water table depletion produced by the drilling of the TT was estimated between 15 and 120 m above the tunnel, and between 60 and 100 m in the central sector of the Alcadozo aquifer, W of the tunnel. The flow seems stable since the early 2000s, with a current average discharge around Q ≈ 100 L/s. A volume of about 340 hm^3 has been drained into the tunnel in the period 1969-2016.

The average depletion coefficient estimated for the tunnel, $\alpha_{TT} = 9.76 \cdot 10^{-5}$ d^{-1} (regional-subregional scale), and for the main permanent springs in the area, $\alpha_S = 3.5 \cdot 10^{-3}$ d^{-1} (subregional-local scale), differ in a factor of 100, but they are consistent with the different spatial scales of the massif volumes involved in both cases, which correspond to an order of magnitude ($10^2 = 100$). The ratio varies according to the dimension squared. The magnitude of α_{TT} shows a large volume of groundwater reserves ($1/\alpha_{TT} \approx 30$ yr) and a good regulation capacity of the aquifer volume that discharged to the tunnel since its drilling; the magnitude of $1/\alpha_S \approx 0.8$ yr shows smaller volumes of aquifer contributing to the main springs.

Looking at the position of the hydrographic divide between the basins of the Júcar and the Segura rivers, on the northern part of the tunnel, around 65 % of the groundwater inflows come from groundwater recharged in the Segura hydrographic basin and 35 % come from the Júcar basin. However, considering that the position of the hydrogeological divide is displaced several km to the N of the hydrographic one, all groundwater inflows come from the "hydrogeological" basin of the Segura river. This is a main finding of this work.

Major ion data, main physic-chemical characteristics, water stable isotope ($\delta^{18}O$ and $\delta^{2}H$) contents and tritium activities (^{3}H) of the main groundwater inflows to the tunnel allows identifying two different inflow composition groups, which suggest two main sources. One group is located in the central part of the tunnel and the other is in the southern sector. An isotopic mass balance shows that the inflows of the central sector contribute about 75 % of the total inflow to the tunnel, and the remaining 25 % come from the southern sector.

The joint analysis of the stable isotopes, the regional altitudinal isotopic gradient, the ^{3}H activities (0.4 to 2.3 ± 0.2 TU), and the chemical composition of the water draining to the central sector of the tunnel (calcium-carbonate chemical type; EC ≈ 600 µS/cm), shows that those inflows are mixtures of local (≈ 5-10 km) and regional groundwater flow lines (≈ 30-40 km to the NW of the tunnel) through limestones. The origin of the inflows located on the southern sector of the tunnel is not fully explained. Their stable isotope composition suggests a sub-regional origin (≈20 km to the NW), but their reduced mineralization (EC ≈ 430 µS/cm), small Cl^{-} (≈ 10 mg/L) and relatively high NO_3^{-} concentrations (14 -39 mg/L), and the possible evaporative enrichment in the stable isotopes point to rather local flows with contribution of excess irrigation water from nearby agricultural soils. However, the low tritium contents of these inflows (0.2 to 0.5 ± 0.1 TU) are not consistent with local origin and/or short transit times. Therefore, recharge through relatively thick, porous media should be considered in future fieldwork.

This study shows that total discharge to the TT has been stable since around twenty years ago. Former studies showed that discharges in the main springs in the nearby area have been also stable for more than fifteen years. New hydrodynamic changes are on the horizon, as the 2021-2027 Segura river Basin Water Plan considers allowing new irrigation systems using groundwater (≤10 hm^3/year), for rural socioeconomic development of the area. This will imply the administrative allocation of the renewable groundwater resources in the aquifers involved, whose natural discharge to springs and the Mundo river, and predictably also to the TT, will be reduced. The work is an example of how a sound review and elaboration of simple historical data such as total groundwater inflow volumes, integrated with more sophisticated data, but currently of common use, such as isotopic values, can provide robust conceptual models on the long term modification of regional groundwater levels and discharge flow due to a disturbance performed several decades ago. The findings of this study are relevant to forecast the expected evolution of the piezometric levels and of groundwater discharge to springs and the tunnel due to the drilling of new wells.

A sound prediction of the impacts of anthropogenic or other type of changes (i.e. climate change) on the aquifer balance and the magnitude of modifications requires a good conceptual model supported by groundwater flow modelling, calibrated with long time series of hydrogeological data. Thus, monitoring groundwater levels, discharge to the tunnel, and the chemical and isotopic composition of groundwater should be continued and complemented by new adequate observation networks.

The results and how to attain them are relevant in international and regional transboundary cases involving agreements and possible compensations for unaccounted groundwater transfers, especially in water scarce arid and semiarid areas with water demand close to available resources, including ecosystems and rights of local populations. This is also important when combining surface water planning with aquifer management, as the boundaries may not coincide in detail and direct and indirect groundwater exploitation may displace the groundwater boundary, which is difficult to be observed.

Acknowledgements

This study is part of the work undertaken under projects REDESAC (CLG2009-12910-C03), funded by the Spanish Ministry of Science and Innovation, and ALCAMOD (grant No. 2099) and “Networks Control and Infrastructures” (grant No. 2823), funded by the Geological Survey of Spain. The authors thank the Tajo river Basin Authority for providing basic historical information and data, and the two anonymous reviewers that contributed to improve the work.

References

Alcalá, F.J., Custodio, E., 2004. La deposición atmosférica de cloruro al terreno en España. Bol Geol Min. Madrid. 115 (esp): 319–329. ISSN: 0366–0176 (In Spanish).

Alcalá, F.J., Custodio, E., 2008a. Atmospheric chloride deposition in continental Spain. Hydrol Process. 22: 3636–3650.

Alcalá, F.J., Custodio, E., 2008b. Using the Cl/Br ratio as a tracer to identify the origin of salinity in aquifers in Spain and Portugal. J Hydrol. 359: 189–207.

Alcalá, F.J., Custodio, E., 2012. Spatial average recharge through atmospheric chloride mass balance and its uncertainty in continental Spain. Hydrol Process. 28: 218–236.

Alcalá, F.J., Custodio, E., 2015. Natural uncertainty of spatial average aquifer recharge through atmospheric chloride mass balance in continental Spain. J Hydrol. 524: 642-661.

Araguás-Araguás, L.J., 1991. Adquisición de los contenidos isotópicos (^{18}O y ^{2}H) de las aguas subterráneas: variaciones en la atmósfera y en la zona no saturada del suelo. Tesis Doctoral. Universidad Autónoma de Madrid: 1- 286 (In Spanish).

Attanayake, P.M., Waterman, M.K., 2006. Identifying environmental impacts of underground construction. Hydrogeol J. 14: 1160-1170.

Azema, J., Foucault, A., Fourcade, E., García Hernández. M,, González Donoso, J.M., Linares, A., Linares, D., López Garrido, A.C., Rivas, P., Vera, J.A., 1979. La microfacies del Jurásico y Cretácico de las Cordilleras Béticas. Universidad de Granada: 1- 83 (In Spanish).

Baena, J., Jerez, L., 1982. Síntesis para un ensayo paleogeográfico entre la Meseta y la Zona Bética S. (s.str). Colección Informe, ITGE. Madrid: 1- 256 (In Spanish).

Bagnoli, P., Bonfanti, M., Della Vecchia, G., Lualdi, M., Sgambi, L., 2015. A method to estimate concrete hydraulic conductivity of underground tunnel to assess lining degradation. Tunnelling Underground Space Technol. 50: 415-423.

Butscher, C., 2012 Steady-state groundwater inflow into a circular tunnel. Tunnelling Underground Space Technol. 32: 158-167.

Butscher, C., Huggenberger, P., Zechner, E., 2011. Impact of tunneling on regional groundwater flow and implications for swelling of clay-sulfate rocks. Eng Geol. 117: 198-206.

Carrera, J., Vázquez-Suñé, E., 2008. Sobre la interacción entre acuíferos y obras subterráneas. El agua y las Infraestructuras en el Medio Subterráneo. Publicaciones del Instituto Geológico y Minero de España Madrid. ISBN: 978–84–7840–807–8 (In Spanish).

Castaño, S., Rodríguez-Arévalo, J., 2019. Mapping environmental tritium activity concentration in recent precipitation in Spain to trace moisture sources in the hydrological cycle. International Symposium on Isotope Hydrology: Advancing the Understanding of Water Cycle Processes; DOI:10.13140/RG.2.2.31222.04165.

CHJ., 2016. Plan Hidrológico de la cuenca del Júcar, periodo 2015-2021. R.D. 1/2016 de 8 de enero, BOE de 19 de enero de 2016. https://www.chj.es/es-es/medioambiente/planificacionhidrologica/Paginas/PHC-2015-2021-Plan-Hidrologico-cuenca.aspx/ (In Spanish) (accesed 20 December 2020).

CHS., 2016. Plan Hidrológico de la cuenca del Segura, periodo 2015-2021. R.D. 1/2016 de 8 de enero, BOE de 19 de enero de 2016. https://www.chsegura.es/chs/planificacionydma/planificacion15-21/ (In Spanish) (accesed 20 December 2020).

CHS., 2020. Esquema de temas importantes de la Demarcación Hidrográfica del Segura 2021-2027. https://www.chsegura.es/es/cuenca/planificacion/planificacion-2021-2027/el-proceso-de-elaboracion/ (In Spanish) (accesed 20 December 2020).

Chiocchini, U., Castaldi, F., 2011. The impact of groundwater on the excavation of tunnels in two different hydrogeological settings in central Italy. Hydrogeol J. 19: 651-669.

Chiu, Y-C., Chia, Y., 2012. The impact of groundwater discharge to the Hsueh-Shan tunnel on the water resources in northern Taiwan. Hydrogeol J. 20: 1599-1611.

Clark, I., 1997. Fritz P. Environmental isotopes in hydrogeology. Lewis Publishers. Boca Ratón, USA, 1- 328.

Craig, H., 1961. Isotopic variations in meteoric waters. Science. 133: 1702-1703.

Custodio, E., 2009. Las galerías de agua del macizo de Famara (Lanzarote): aspectos hidráulicos e hidrogeoquímicos en el entorno de 1970. El Agua y las Infraestructuras en el Medio Subterráneo. Publicaciones del Instituto Geológico y Minero de España Madrid. 123–129. ISBN: 978–84–7840–807–8 (In Spanish).

Custodio, E., Llamas, M.R., 1976. Hidrología subterránea. Ediciones Omega, Barcelona, 1-2350.

Custodio, E., Herrera, C., 2000. Utilización de la relación Cl/Br como trazador hidrogeoquímico en hidrología subterránea. Bol Geol Min. 111(4): 49–68 (In Spanish).

Custodio, E., Jódar, J., 2016. Simple solutions for steady–state diffuse recharge evaluation in sloping homogeneous unconfined aquifers by means of atmospheric tracers. J Hydrol. 540: 287–305.

Fallot, P., 1948. Les Cordillères Bétiques. Estudios Geológicos; 4:83-172 (In French).

Farhadian, H., Aalianvari, A., Katibeh, H., 2012. Optimization of analytical equations of groundwater seepage into tunnels: A case study of Amirkabir tunnel. J Geol Soc India. 80: 96-100.

Farhadian, H., Nikvar-Hassani, A., 2019. Water flow into tunnels in discontinuous rock: a short critical review of the analytical solution of the art. Bull Eng Geol Environ. 78: 3833-3849.

Fernández, G., Moon, J., 2010. Excavation-induced hydraulic conductivity reduction around a tunnel - Part 1: Guideline for estimate of ground water inflow rate. Tunnelling Underground Space Technol. 25: 560-566.

Font-Capó, J., Vázquez-Suñé, E., Carrera, J., Marti, D., Carbonell, R., Perez-Estaun, A., 2011. Groundwater inflow prediction in urban tunneling with a tunnel boring machine (TBM). Eng Geol. 121: 46-54.

García Yagüe, A., 1986a. Experiences of the exploration technics in Talave tunnel, Spain. 5th International Congress Association of Engineering Geology, Buenos Aires: 277-281.

García Yagüe, A., 1986b. The Gloria fault in Talave tunnel, Spain. 5th International Congress Association of Engineering Geology, Buenos Aires: 283-290.

Gattinoni, P., Scesi, L., 2010. An empirical equation for tunnel inflow assessment: application to sedimentary rock masses. Hydrogeol J. 18: 1797-1810.

Goodman, R.F., Moye, D.G., van Schaikwyk, A., Javandel, I., 1965. Ground water inflows during tunnel driving. 2. Bull Int Assoc Eng Geol. 39-56.

Hassani, A.N., Farhadian, H., Katibeh, H., 2018. A comparative study on evaluation of steady-state groundwater inflow into a circular shallow tunnel. Tunnelling Underground Space Technol. 73: 15-25.

Herschy, R. 1993. The velocity-area method. Flow Measurement and Instrumentation. 4(1): 7-10.

Hornero, J., 2018. Contribución de las técnicas hidroquímicas, isotópicas e hidrodinámicas a la caracterización de acuíferos carbonatados y su relación con la red de flujo superficial. Aplicación al acuífero de Alcadozo (cuenca del Segura). Tesis doctoral. Universidad Politécnica de Cartagena:1-315. https://dx.doi.org/10.31428/10317/7044 (In Spanish).

Hornero, J., Manzano, M., Ortega, L., Custodio, E., 2016. Integrating soil water and tracer balances, numerical modelling and GIS tools to estimate regional groundwater recharge: Application to the Alcadozo Aquifer System (SE Spain). Sci Total Environ. 568: 415-432.

Huang, Y., Yu, Z., Zhou, Z., 2013. Simulating groundwater inflow in the underground tunnel with a coupled fracture-matrix model. J Hydrol Eng. 18: 1557-1561.

Hwang, J-H,, Lu, C-C., 2007. A semi-analytical method for analyzing the tunnel water inflow. Tunnelling Underground Space Technol. 22: 39-46.

IGME., 2005. Modelo matemático de flujo de la Unidad Hidrogeológica 08.29 Mancha-Oriental. http://www.igme.es/ (In Spanish) (accesed 18 October 2020).

IGME-CHS., 2009. Definición de un plan de extracciones en la cuenca alta del Segura en épocas de sequía. Instituto Geológico y Minero de España. http//:www.igme.es (In Spanish) (accesed 18 October 2020)

IGME-DGA., 2012. Las aguas subterráneas en la planificación hidrológica. Instituto Geológico y Minero de España.:1-481 http://www.mapama.gob.es/es/agua/publicaciones/AGUAS_SUBTERRANEAS_1de7_tcm7-213349.pdf (In Spanish) (accesed 18 October 2020).

Jerez Mir, L., 1973. Geología de la zona Prebética en la transversal de Elche de la Sierra y sectores adyacentes (provincias de Albacete y Murcia). Tesis doctoral. Facultad de Ciencias. Universidad de Granada (In Spanish).

Jiang, X-W., Wan, L., Yeh, T-CJ., Wang , X-S,, Xu, L., 2010. Steady-state discharge into tunnels in formations with random variability and depth-decaying trend of hydraulic conductivity. J Hydrol. 387: 320-327.

Jiménez–Martínez, J., Custodio, E., 2008. El exceso de deuterio en la lluvia y en la recarga a los acuíferos en el área circum–mediterránea y en la costa mediterránea española. Bol Geol Min. 119(1): 21–32 (In Spanish).

Jin, X., Liu, H., Zhou, S., 2012. Research of water inflow impact on ecological environment for Cimushan tunnel. In: Wang LH, Xu G, editors. Advances in Industrial and Civil Engineering, Pts 1-4. 594-597: 1263-1268.

Kolymbas, D., Wagner, P., 2007. Groundwater ingress to tunnels - The exact analytical solution. Tunnelling Underground Space Technol. 22: 23-27.

Li, D., Li, X., Li, CC., Huang, B., Gong, F., Zhang, W., 2009. Case studies of groundwater flow into tunnels and an innovative water-gathering system for water drainage. Tunnelling Underground Space Technol. 24: 260-268.

Li, P., Wang, F., Long, Y., Zhao, X., 2018. Investigation of steady water inflow into a subsea grouted tunnel. Tunnelling Underground Space Technol. 80: 92-102.

Liu, D., Yang, LZ., Mao, J., 2000. Application of environmental isotope to groundwater study of the Qinling Railway tunnel. Tunnelling Underground Space Technol. 15: 147-151.

Liu, J., Liu, D., 2015. Identification of the water resources of tunnel inflow based on a stable isotopes mass balance model. 52. Mod Tunnelling Technol. 106-110.

Liu, J., Liu, D., Songk, K., 2015. Evaluation of the influence caused by tunnel construction on groundwater environment: A case study of Tongluoshan Tunnel, China. Adv Mater Sci Engin. https://doi.org/10.1155/2015/149265.

Liu, TK., Chen, CH., Yang, TF., Lee, M., 2005. Tritium concentrations and radiocarbon ages of gushing groundwater from Hsuehshan Tunnel, northern Taiwan. Terr Atmos Ocean Sci. 16: 909-917.

Marechal, J-C., 2012. The Mont-Blanc road tunnel: example of groundwater observatory in the Alps. Houille Blanche-Revue Internationale De L Eau: 44-50.

Marechal, J-C., Lanini, S., Aunay, B., Perrochet, P., 2014. Analytical solution for modeling discharge into a tunnel drilled in a heterogeneous unconfined aquifer. Ground Water. 52: 597-605.

Marechal, JC., Etcheverry, D., 2003. The use of ^{3}H and ^{18}O tracers to characterize water inflows in Alpine tunnels. Appl Geochem. 18: 339-351.

Menéndez-Pidal de Navascues, I., 2006. Interacción de las arenas en Facies Utrillas en las obras de ingeniería civil. Revisión documental y caracterización geológico-geotécnica.Tesis doctoral. Universidad Politécnica de Madrid: 1- 308 (In Spanish).

Moon, J-S., Zheng, A-Q,, Jang, S.. 2017. Assessment of groundwater inflow rate into a tunnel considering groundwater level drawdown and permeability reduction with depth. J Korean Tunnelling Underground Space Assoc. 19: 109-120.

MOP-DGOH-SGOP., 1967. Anteproyecto general de aprovechamiento conjunto de los recursos hidráulicos del centro y sureste de España. Complejo Tajo-Segura. En: Mendiluce JMM, Gutiérrez JMP, editores. Tomo I. Memoria General, Madrid. (In Spanish).

MOP-DGOH-SGOP., 1982a. Proyecto de estación de aforos en cauce afluente de la Rambla de Talave, 12/82. Ministerio de Obras Públicas-Dirección General de Obras Hidráulicas-Servicio Geológico. (In Spanish).

MOP-DGOH-SGOP., 1982b. Estudio geológico del canal de salida del túnel de Talave, 04/82. Ministerio de Obras Públicas-Dirección General de Obras Hidráulicas-Servicio Geológico. (In Spanish).

MOP-DGOH-SGOP., 1983. Trabajos geológicos realizados para el túnel de Talave del Trasvase Tajo-Segura (Albacete), 07/83. Ministerio de Obras Públicas y Urbanismo. Dirección General de Obras Hidráulicas. Servicio Geológico. (In Spanish).

Moral, F., 2005. Contribución al conocimiento de los acuíferos carbonáticos de la Sierra de Segura (Alto Guadalquivir y Alto Segura). Tesis doctoral. Universidad Pablo de Olavide, Sevilla: 1- 580 (In Spanish)

Ofterdinger, US., Renard, P., Loew S., 2014. Hydraulic subsurface measurements and hydrodynamic modelling as indicators for groundwater flow systems in the Rotondo granite, Central Alps (Switzerland). Hydrol Process. 28: 255-278.

Ortega, L., Manzano, M., Custodio, E., Hornero, J., Rodriguez-Arevalo, J., 2015. Using ^{222}Rn to identify and quantify groundwater inflows to the Mundo river (SE Spain). Chem Geol. 395: 67-79.

Oteo, C., 2016. El agua y los túneles. Revista de Obras Públicas (nº 3579): 31-54 (In Spanish).

Park, K-H., Owatsiriwong, A., Lee, J-G., 2008. Analytical solution for steady-state groundwater inflow into a drained circular tunnel in a semi-infinite aquifer: A revisit. Tunnelling Underground Space Technol. 23: 206-209.

Pastorell,i S., Marini, L., Hunziker, J., 2001. Chemistry, isotope values (delta D, delta O-18, delta S-34(SO4)) and temperatures of the water inflows in two Gotthard tunnels, Swiss Alps. Appl Geochem. 16: 633-649.

Perello, P., Baietto, A., Burger, U., Skuk, S., 2014. Excavation of the Aica-Mules pilot tunnel for the Brenner base tunnel: information gained on water inflows in tunnels in granitic massifs. Rock Mech Rock Eng. 47: 1049-1071.

Pérez Crespo, A., 2009. Los orígenes y puesta en marcha del Trasvase Tajo-Segura. Una crónica personal. Murcia. Fundación Instituto Euromediterráneo del Agua, Murcia: 1-359. ISBN: 978-84-936326-5-6 (In Spanish).

Perrochet, P., 2005. Confined flow into a tunnel during progressive drilling: An analytical solution. Ground Water. 43: 943-946.

Perrochet, P., Dematteis, A., 2007. Modeling transient discharge into a tunnel drilled in a heterogeneous formation. Ground Water. 45: 786-790.

Plata, A., 1994. Composición isotópica de las precipitaciones y aguas subterráneas de la península Ibérica, CEDEX, Monografía M-39. ISSN 0221- 8203 0221- 8203 (In Spanish).

RAEMIA., 2019. Recarga natural a los acuíferos, metodología y soporte de la isotopía del agua. Aplicación a la planificación hidrológica y conocimiento de las aguas subterráneas en España (Aquifer natural recharge, methodology and water isotopes support. Application to water planning and groundwater knowledge in Spain). 1-1206. E Custodio, with contributions of J Jódar, JV Giráldez and A Sahuquillo. http://hdl.handle.net/2117/182282.

Raposo, R., Molinero, J., Dafonte, J., 2010. Quantitative evaluation of hydrogeological impact produced by tunnel construction using water balance models. Eng Geol. 116: 323-332.

Rodríguez Estrella, T., 1979. Geología e hidrogeología del sector Alcaráz-Liétor-Yeste (Provincia de Albacete). Síntesis Geológica de la Zona Prebética. Instituto Geológico y Minero de España. (In Spanish).

Sauer, VB., Meyer, RW., 1992. Determination of error in individual discharge measurements. U.S. Geological. Survey: 92–144.

Scanlon, BR., Keese, KE., Flint, AL., Flint, LE., Gaye, CB., Edmunds, WM., 2006. Global synthesis of groundwater recharge in semiarid and arid regions. Hydrol Process. 20: 3335-3370.

Sharifzadeh, M., Karegar, S., Ghorbani, M., 2013. Influence of rock mass properties on tunnel inflow using hydromechanical numerical study. Arabian J Geosci. 6: 169-175.

Sophocleous, M., 1992. Groundwater recharge estimation and regionalization The Great Bend Prairie of Central Kansas and its recharge statistics. J Hydrol. 137: 113-140.

Su, K., Zhou, Y., Wu, H., Sh,i C., Zhou, L., 2017. An analytical method for groundwater inflow into a drained circular tunnel. Ground Water. 55: 712-721.

Tomonaga, Y., Marzocchi, R., Pera, S., Pfeifer, H-R., Kipfer, R., Decrouy, L., et al., 2017. Using noble-gas and stable-isotope data to determine groundwater origin and flow regimes: Application to the Ceneri Base Tunnel (Switzerland). J Hydrol. 545: 395-409.

Tsang, CF., Niemi, A., 2013. Deep hydrogeology: a discussion of issues and research needs. Hydrogeol J. 21: 1687–1690.

Vincenzi, V., Gargini, A., Goldscheider, N., Piccinini, L., 2014. Differential hydrogeological effects of draining tunnels through the Northern Apennines, Italy. Rock Mech Rock Eng. 47: 947-965.

Walton-Day, K., Poeter, E., 2009. Investigating hydraulic connections and the origin of water in a mine tunnel using stable isotopes and hydrographs. Appl Geochem. 24: 2266-2282.

Xiao, Y., Hao, Q., Shao, J., Cui, Y., Zhang, Q., 2019. Numerical simulation for impacts of mountainous tunnel drainage on groundwater environment. Sustainable Development of Water Resources and Hydraulic Engineering in China: 219-226.

Xie, H-s.,Jiang, C., He, J-l., Han, H-x., 2019. Analytical solution for the steady-state karst water inflow into a tunnel. Geofluids. 9 pages. https://doi.org/10.1155/2019/1756856.

Yoo, C., Lee, Y., Kim, S-H., Kim, H-T., 2012. Tunnelling-induced ground settlements in a groundwater drawdown environment - A case history. Tunnelling Underground Space Technol. 29: 69-77.

Zarei, HR., Uromeihy, A., Sharifzadeh, M., 2011. Evaluation of high local groundwater inflow to a rock tunnel by characterization of geological features. Tunnelling Underground Space Technol. 26: 364-373.

Zhang, Z., Xu, P., Zhang, H., Zhang, K., 2019. Dynamic Change Characteristics of Groundwater Affected by Super-Long Tunnel Construction in the Western Mountainous Area of China. Sustainability. 11: 2329. https://doi.org/10.3390/su11082329.

Table 1. Annual water inflow volume to the Talave tunnel for the period 1981-2012, measured at the southern output. Source: DTST-CHT.

Year	Water inflow volume (hm^3/year)	Average water inflow (L/s)	Year	Water inflow volume (hm^3/year)	Average water inflow (L/s)
1984	8.36	265	1999	4.33	137
1985	9.53	302	2000	3.90	124
1986	8.86	281	2001	3.55	113
1987	8.12	257	2002	3.93	125
1988	8.16	259	2003	4.58	145
1989	6.58	209	2004	4.77	151
1990	6.53	207	2005	4.20	133
1991	7.39	234	2006	3.54	112
1992	6.30	200	2007	3.39	107
1993	6.04	191	2008	3.67	116
1994	5.70	181	2009	3.28	104
1995	5.23	166	2010	3.48	110
1996	5.27	167	2011	3.99	126
1997	5.18	164	2012	3.89	123
1998	4.12	131			

Table 2. Gauged water flow rates and estimated yearly volumes at the exit of the Talave tunnel in different dates. For date 29/10/2014, the flow rate measured inside the tunnel just in the Segura-Júcar basins divide is also shown. Source: own data.

Date	Water flow in the Segura-Júcar basins divide (L/s)	Uncertainty (± 2σ)* (L/s)	Total flow at the exit of the tunnel (L/s)	Uncertainty (± 2σ)* (L/s)	Estimated water inflow volume (hm^3/yr)	Uncertainty (± 2σ) (hm^3/yr)
29/10/2014	50.65	14.58	146.77	20.82	4.61	0.65
10/04/2015	-	-	87.10	12.96	2.75	0.41
03/02/2016	-	-	65.23	9.70	2.21	0.33
24/10/2016	-	-	70.21	10.53		
02/03/2017	-	-	91.40	8.91	2.89	0.28

(*) According to Sauer and Meyer (1992)

Table 3. Physic-chemical values and isotopic contents of the water inflows sampled inside the tunnel (149 to 155) and of total flow at the outlet (125).

ID	Sampling date	EC lab. (µS/cm)	pH lab.	Cl^- (mgL^{-1})	SO_4^{2-} (mgL^{-1})	HCO_3^- (mgL^{-1})	NO_3^- ($mg L^{-1}$)	Na^+ (mgL^{-1})	Mg^{2+} (mgL^{-1})	Ca^{2+} (mgL^{-1})	K^+ (mgL^{-1})	Br^- (mgL^{-1})	Cl/Br (molar)	$\delta^{18}O$ (‰ VSMOW)	δ^2H (‰ VSMOW)	d(‰)	$^3H \pm 1\sigma$ (TU)
149	28/10/2014	610	7.71	26.8	26	338	31	16	38	76	2.0	0.107	564	-8.06	-53.97	10.49	0.40 ± 0.20
150	28/10/2014	601	7.61	16.9	69	308	19	14	33	84	1.0	0.070	545	-8.16	-54.09	11.17	1.10 ± 0.20
151	28/10/2014	578	7.89	21.3	59	293	25	16	36	72	2.0	0.085	565	-8.06	-53.70	10.78	2.30 ± 0.20
152	28/10/2014	599	7.75	19.0	23	358	21	14	41	71	0.0	0.099	432	-7.90	-52.62	10.60	0.90 ± 0.20
153	28/10/2014	607	7.80	19.6	32	362	20	14	35	86	0.0	0.102	433	-7.92	-52.70	10.69	1.30 ± 0.20
154	28/10/2014	423	7.94	9.0	15	222	39	10	27	48	0.0	0.093	219	-6.32	-44.97	5.56	0.50 ± 0.10
155	28/10/2014	432	7.87	13.2	7	272	14	10	32	47	0.0	0.070	426	-7.22	-48.00	9.79	0.20 ± 0.10
125b	28/10/2014	531	7.98	20.6	51	263	23	16	36	58	2.0	0.093	500	-7.69	-52.28	9.24	1.80 ± 0.20
125a	31/10/2012	497	7.96	19.2	65	253	18	14	37	56	2.0	0.091	475	-7.83	-52.43	10.21	0.90 ± 0.40
125c	10/04/2015	480	7.79	22.0	56	221	18	16	35	48	2.0	0.078	637	-7.85	-53.47	9.31	1.40 ± 0.60
125d	03/02/2016	488	7.79	19.2	55	227	19	16	35	48	2.0	0.079	547	-7.63	-51.61	9.44	0.80 ± 0.30
125e	24/10/2016	499	7.74	18.5	56	231	18	16	34	51	2.0	0.077	542	-7.77	-53.55	8.62	1.30 ± 0.40

Table 4. Estimated relative contribution of the main water inflows from the central and southern sectors of the tunnel to the total water outflow (sample 125) in October 2014.

Water sample	^3H (TU)	$\delta^{18}O$ (‰)	δ^2H (‰)
CSE (Central Sector end-member). Sample 151	2.30	-8.06	-53.70
SSE (Southern Sector end-member). Sample 155	0.20	-7.22	-48.00
MW (Mix Water). Sample 125b	1.80	-7.69	-52.28
MW= X (CSE) + (1-X) SSE			
Fraction of CSE in 125b	0.76	0.56	0.75
Fraction of SSE in 125b	0.24	0.44	0.25

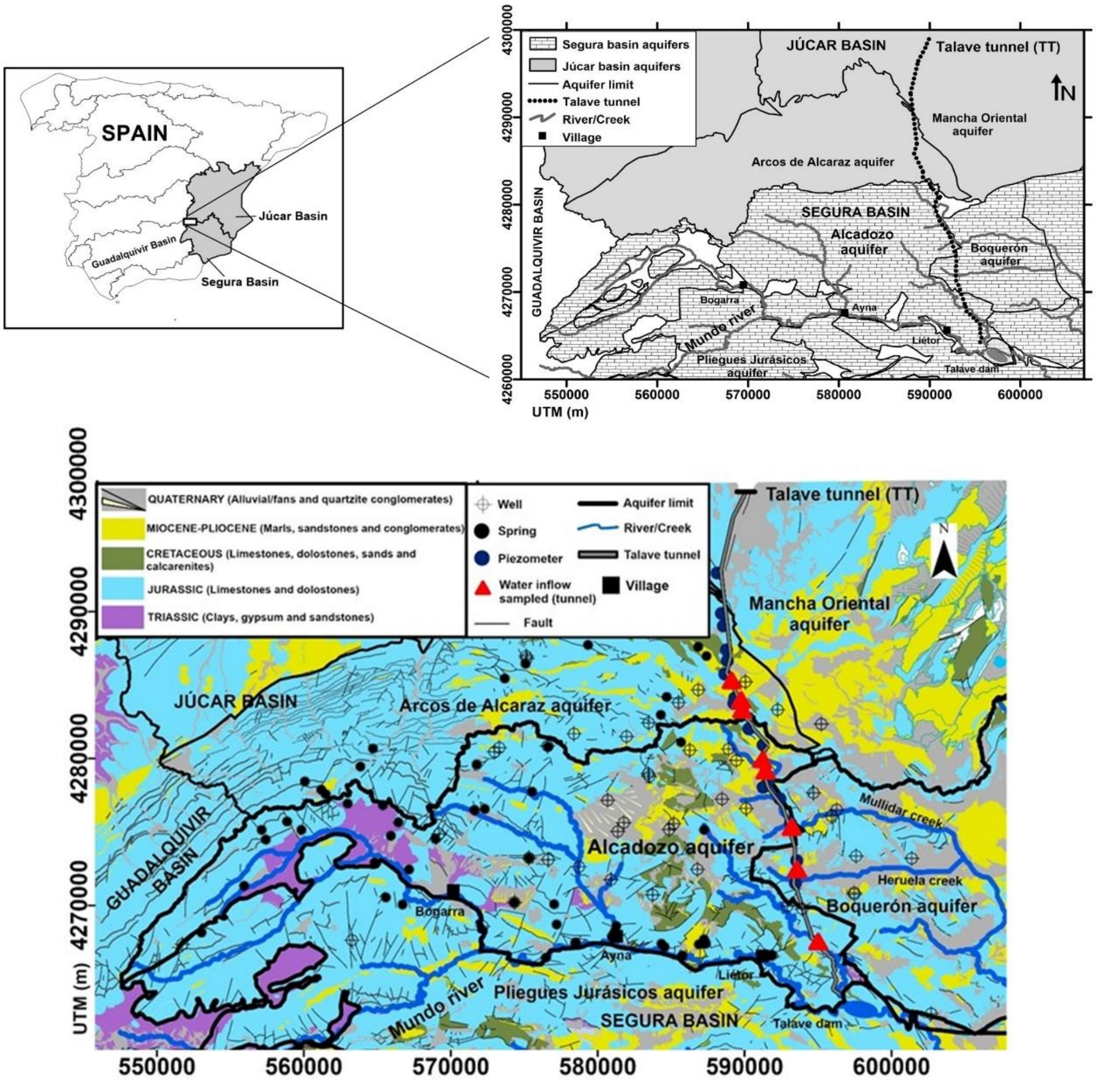

Figure 1. Geological map with location of the Talave tunnel (TT), main villages, Mundo river and creeks, Talave dam, aquifers and hydrographic basins in the study area. Also shown are the sampling points inside the tunnel, and the wells, boreholes and springs studied in former works by the authors and whose data area are used here as complements.

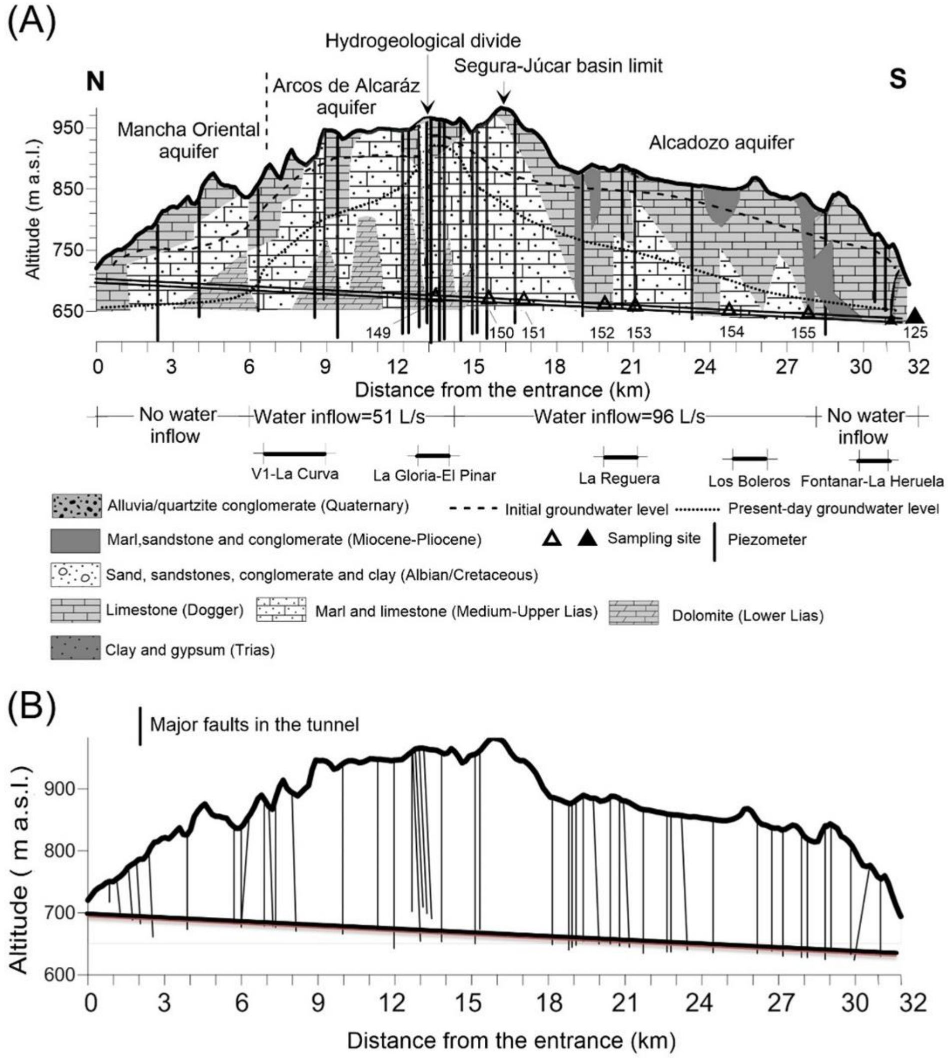

Figure 2. (A) Geological cross-section of the Talave tunnel showing the inferred groundwater level changes caused by its construction, critical hydrogeological zones along the tunnel, location of the main water inflow sites, sampling sites in October 2014, and groundwater inflow rates measured in the same date. The initial groundwater level represents the situation in 1968, and the present-day groundwater level represents the situation since 2014. (B) Major faults crossed by the tunnel. See location in Figure 1.

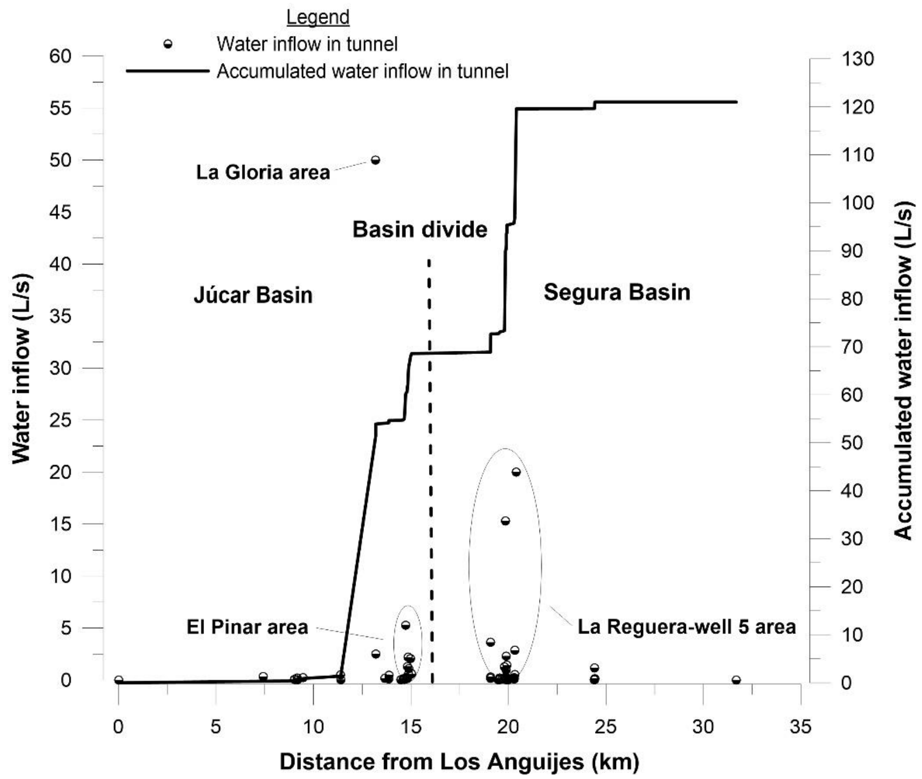

Figure 3. Evolution of total water inflow along the Talave tunnel in December 29, 1999, and location of the main water a point or short length water inflows. Distance from the entrance at Los Anguijes.

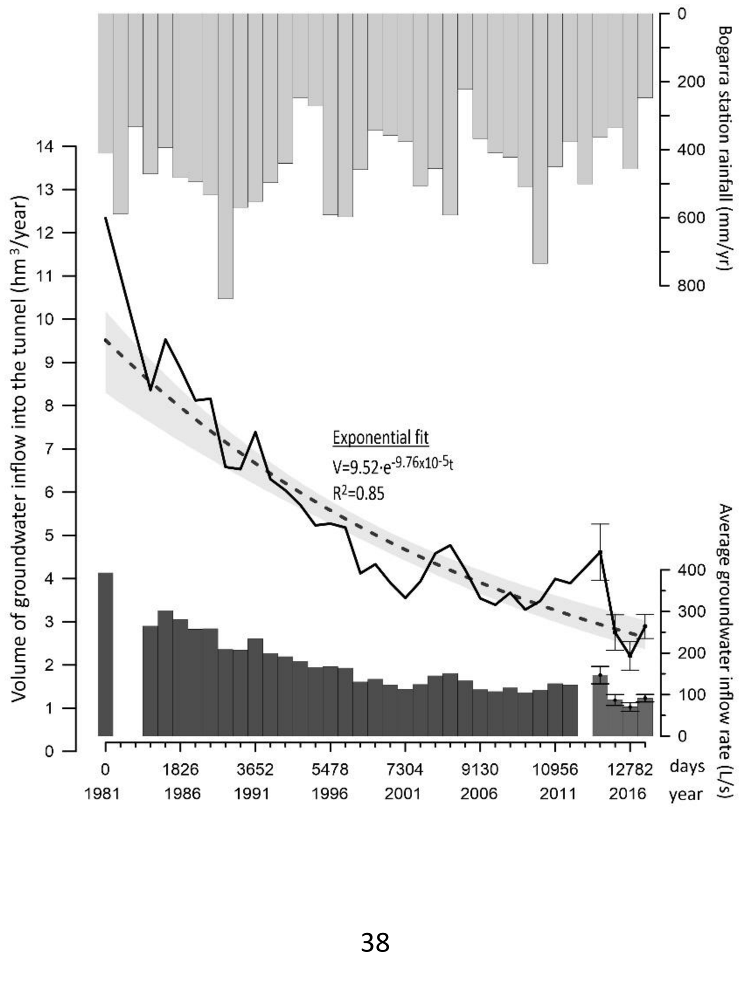

Figure 4. Annual evolution of the total groundwater inflow to the Talave tunnel in the period 1981-2016 (hm^3/year), exponential fit and confidence range. The average water inflow rate (in L/s) and the annual rainfall (mm/yr) in the reference station (Bogarra) are also indicated. Source: elaborated from data provided by the Technical Head of the Tajo Basin Water Authority (water inflow drained and average water inflow), Spanish Agency of Meteorology (pluviometry) and own data (total drainage at the tunnel exit and average water inflow for the period 2014-2016, with the estimated ±2σ uncertainty strip).

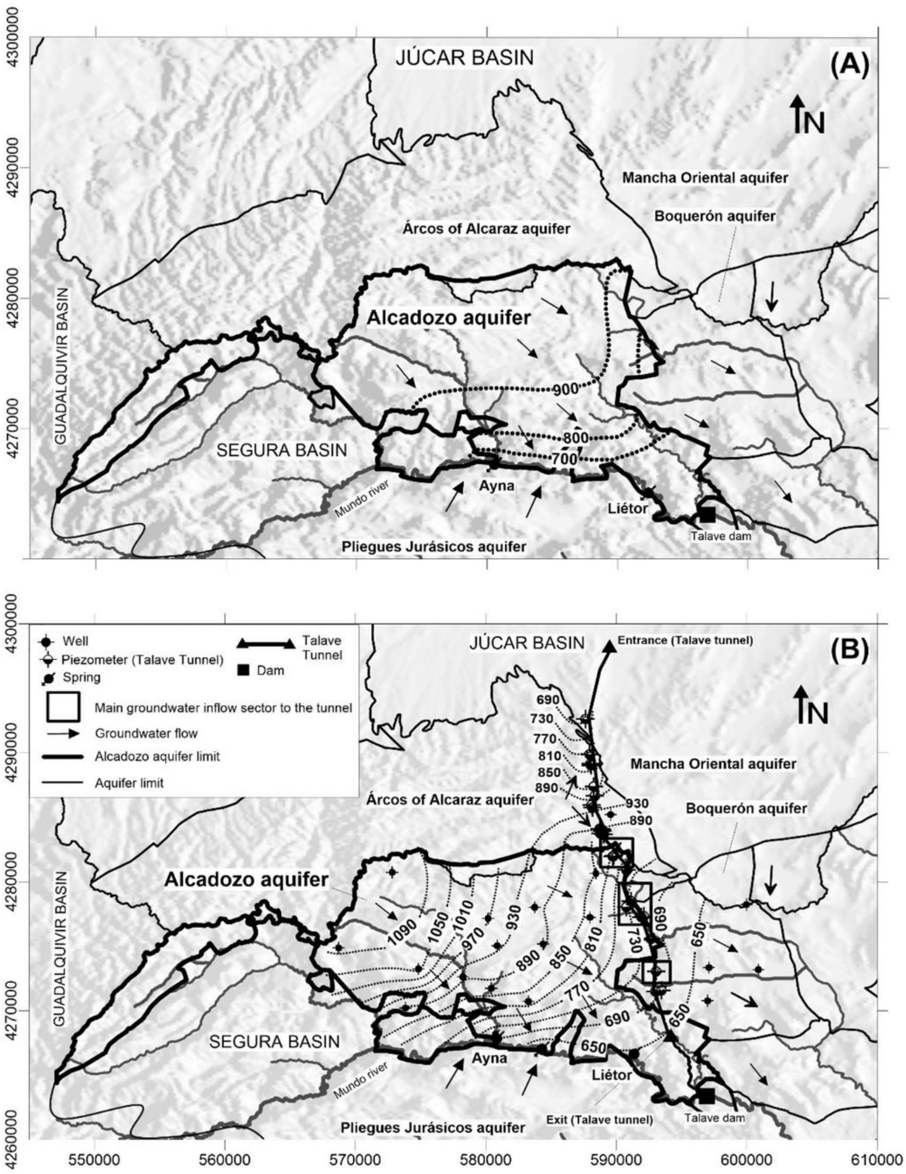

Figure 5. Regional piezometry of the study area in different times. (A) Natural regime in the Alcadozo aquifer before drilling the tunnel (modified from IGME-DGA, 2012). (B) Period 2009-2014, with piezometric data from the Alcadozo aquifer and from the Talave tunnel (own data). The measurement points are shown.

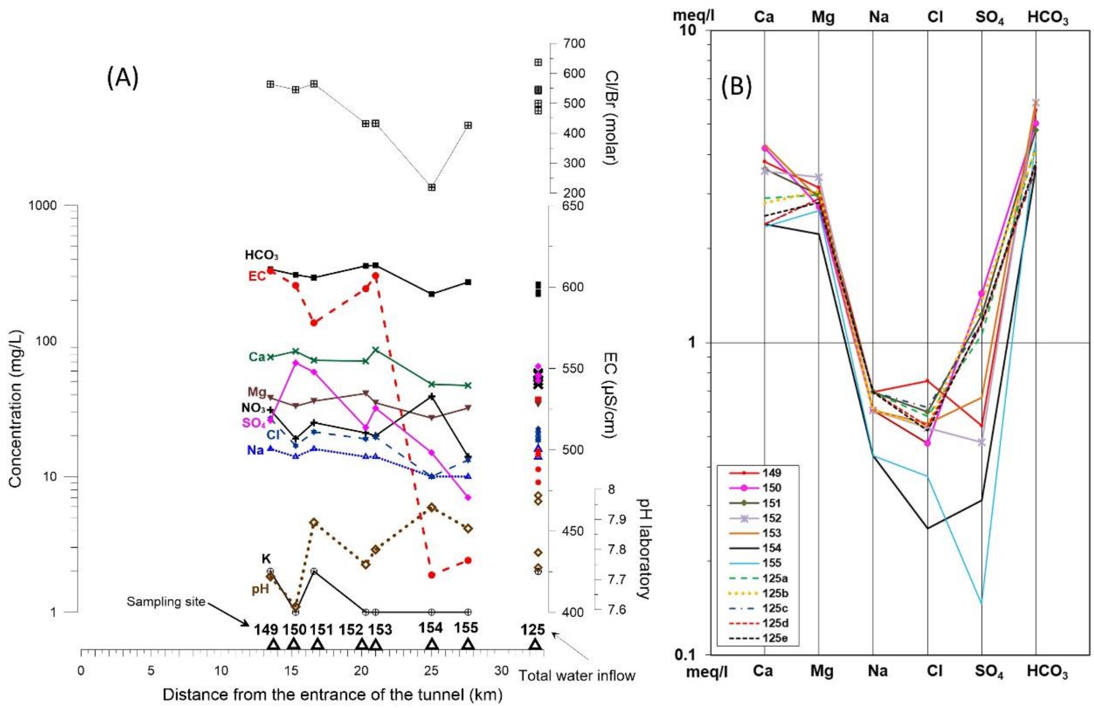

Figure 6. (A) Evolution of major ion concentrations, electrical conductivity (EC), pH, and Cl/Br molar ratio values in seven individual groundwater inflows taken in October 2014 along the Talave tunnel (samples 149 to 155) and in sample 125 of total flow taken at the southern exit of the tunnel, as well as in site 125 in October 2012, April 2015, February 2016 and October 2016. (B) Schoeller-Berkaloff diagram of the chemical composition of the same samples. Modified from Hornero (2018).

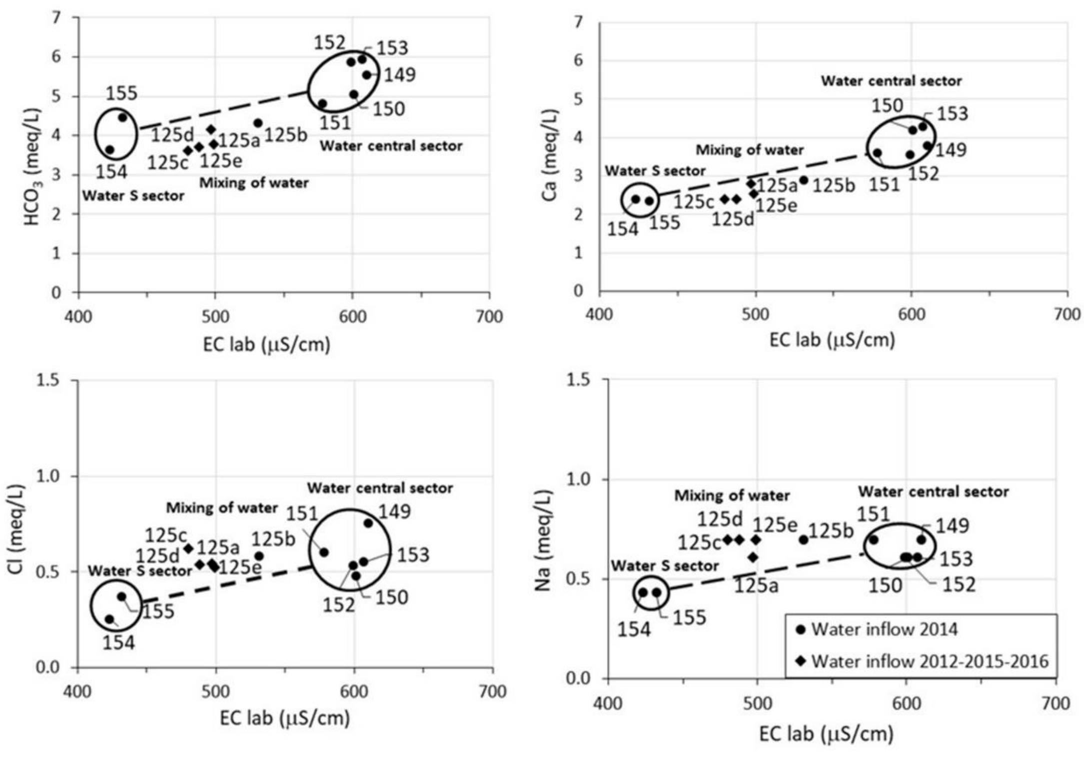

Figure 7. Concentrations of some major solutes (HCO_3^-, Ca^{2+}, Cl^- and Na^+, in meq/L) versus EC (µS/cm) in water sampled inside the tunnel in October 2014 (149 to 155) and at the tunnel exit in different years (125a to e). The figures show the existence of two main chemical groups contributing water to the tunnel, one in the central sector and another in the southern sector. The deviations may be explained by calcite precipitation and additional return irrigation flows.

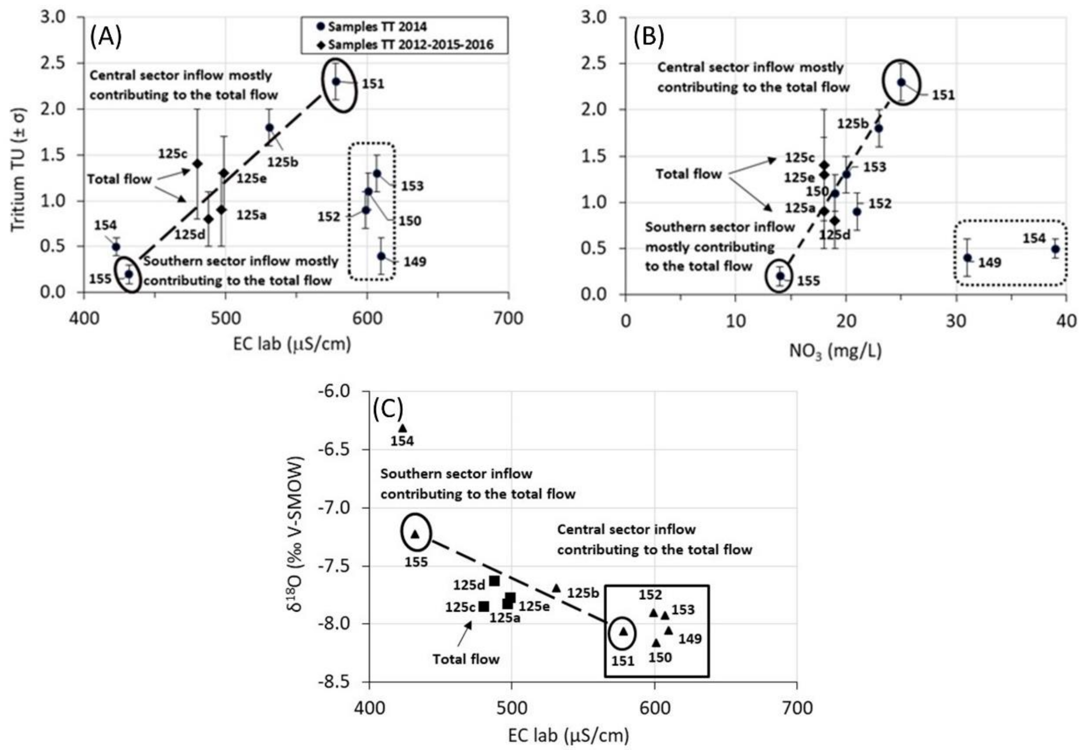

Figure 8. Tritium activity in the water inflow samples taken inside the tunnel (149 to 155) and in total water outflow at the tunnel exit (125) versus (A): Laboratory EC; (B): NO_3^- concentration. It can be observed that the water inflows mainly contributing to the total water outflow from the tunnel are 155 and 151 (circled area), while the contribution of the others (dotted area) is negligible compared to these last ones; (C) $\delta^{18}O$ values measured in the water inflow samples taken inside the tunnel (149 to 155) and in the total water outflow at the tunnel exit (125a to e) versus EC values. Sample 151 has been used as representative of the tunnel central sector end-member.

Table 1. Annual water inflow volume to the Talave tunnel for the period 1981-2012, measured at the southern output. Source: DTST-CHT.

Year	Water inflow volume (hm^3/year)	Average water inflow (L/s)	Year	Water inflow volume (hm^3/year)	Average water inflow (L/s)
1984	8.36	265	1999	4.33	137
1985	9.53	302	2000	3.90	124
1986	8.86	281	2001	3.55	113
1987	8.12	257	2002	3.93	125
1988	8.16	259	2003	4.58	145
1989	6.58	209	2004	4.77	151
1990	6.53	207	2005	4.20	133
1991	7.39	234	2006	3.54	112
1992	6.30	200	2007	3.39	107
1993	6.04	191	2008	3.67	116
1994	5.70	181	2009	3.28	104
1995	5.23	166	2010	3.48	110
1996	5.27	167	2011	3.99	126
1997	5.18	164	2012	3.89	123
1998	4.12	131			

Table 2. Gauged water flow rates and estimated yearly volumes at the exit of the Talave tunnel in different dates. For date 29/10/2014, the flow rate measured inside the tunnel just in the Segura-Júcar basins divide is also shown. Source: own data.

Date	Water flow in the Segura-Júcar basins divide (L/s)	Uncertainty (± 2σ)* (L/s)	Total flow at the exit of the tunnel (L/s)	Uncertainty (± 2σ)* (L/s)	Estimated water inflow volume (hm^3/yr)	Uncertainty (± 2σ) (hm^3/yr)
29/10/2014	50.65	14.58	146.77	20.82	4.61	0.65
10/04/2015	-	-	87.10	12.96	2.75	0.41
03/02/2016	-	-	65.23	9.70	2.21	0.33
24/10/2016	-	-	70.21	10.53		
02/03/2017	-	-	91.40	8.91	2.89	0.28

(*) According to Sauer and Meyer (1992)

Table 3. Physic-chemical values and isotopic contents of the water inflows sampled inside the tunnel (149 to 155) and of total flow at the outlet (125).

ID	Sampling date	EC lab. (µS/cm)	pH lab.	Cl^- (mgL^{-1})	SO_4^{2-} (mgL^{-1})	HCO_3^- (mgL^{-1})	NO_3^- (mg L^{-1})	Na^+ (mgL^{-1})	Mg^{2+} (mgL^{-1})	Ca^{2+} (mgL^{-1})	K^+ (mgL^{-1})	Br^- (mgL^{-1})	Cl/Br (molar)	$\delta^{18}O$ (‰ VSMOW)	δ^2H (‰ VSMOW)	d(‰)	$^3H \pm 1\sigma$ (TU)
149	28/10/2014	610	7.71	26.8	26	338	31	16	38	76	2.0	0.107	564	-8.06	-53.97	10.49	0.40 ± 0.20
150	28/10/2014	601	7.61	16.9	69	308	19	14	33	84	1.0	0.070	545	-8.16	-54.09	11.17	1.10 ± 0.20
151	28/10/2014	578	7.89	21.3	59	293	25	16	36	72	2.0	0.085	565	-8.06	-53.70	10.78	2.30 ± 0.20
152	28/10/2014	599	7.75	19.0	23	358	21	14	41	71	0.0	0.099	432	-7.90	-52.62	10.60	0.90 ± 0.20
153	28/10/2014	607	7.80	19.6	32	362	20	14	35	86	0.0	0.102	433	-7.92	-52.70	10.69	1.30 ± 0.20
154	28/10/2014	423	7.94	9.0	15	222	39	10	27	48	0.0	0.093	219	-6.32	-44.97	5.56	0.50 ± 0.10
155	28/10/2014	432	7.87	13.2	7	272	14	10	32	47	0.0	0.070	426	-7.22	-48.00	9.79	0.20 ± 0.10
125b	28/10/2014	531	7.98	20.6	51	263	23	16	36	58	2.0	0.093	500	-7.69	-52.28	9.24	1.80 ± 0.20
125a	31/10/2012	497	7.96	19.2	65	253	18	14	37	56	2.0	0.091	475	-7.83	-52.43	10.21	0.90 ± 0.40
125c	10/04/2015	480	7.79	22.0	56	221	18	16	35	48	2.0	0.078	637	-7.85	-53.47	9.31	1.40 ± 0.60
125d	03/02/2016	488	7.79	19.2	55	227	19	16	35	48	2.0	0.079	547	-7.63	-51.61	9.44	0.80 ± 0.30
125e	24/10/2016	499	7.74	18.5	56	231	18	16	34	51	2.0	0.077	542	-7.77	-53.55	8.62	1.30 ± 0.40

Table 4. Estimated relative contribution of the main water inflows from the central and southern sectors of the tunnel to the total water outflow (sample 125) in October 2014.

Water sample	^3H (TU)	$\delta^{18}O$ (‰)	δ^2H (‰)
CSE (Central Sector end-member). Sample 151	2.30	-8.06	-53.70
SSE (Southern Sector end-member). Sample 155	0.20	-7.22	-48.00
MW (Mix Water). Sample 125b	1.80	-7.69	-52.28
MW= X (CSE) + (1-X) SSE			
Fraction of CSE in 125b	0.76	0.56	0.75
Fraction of SSE in 125b	0.24	0.44	0.25

Figure

Click here to access/download;Figure;Figura 1.jpg

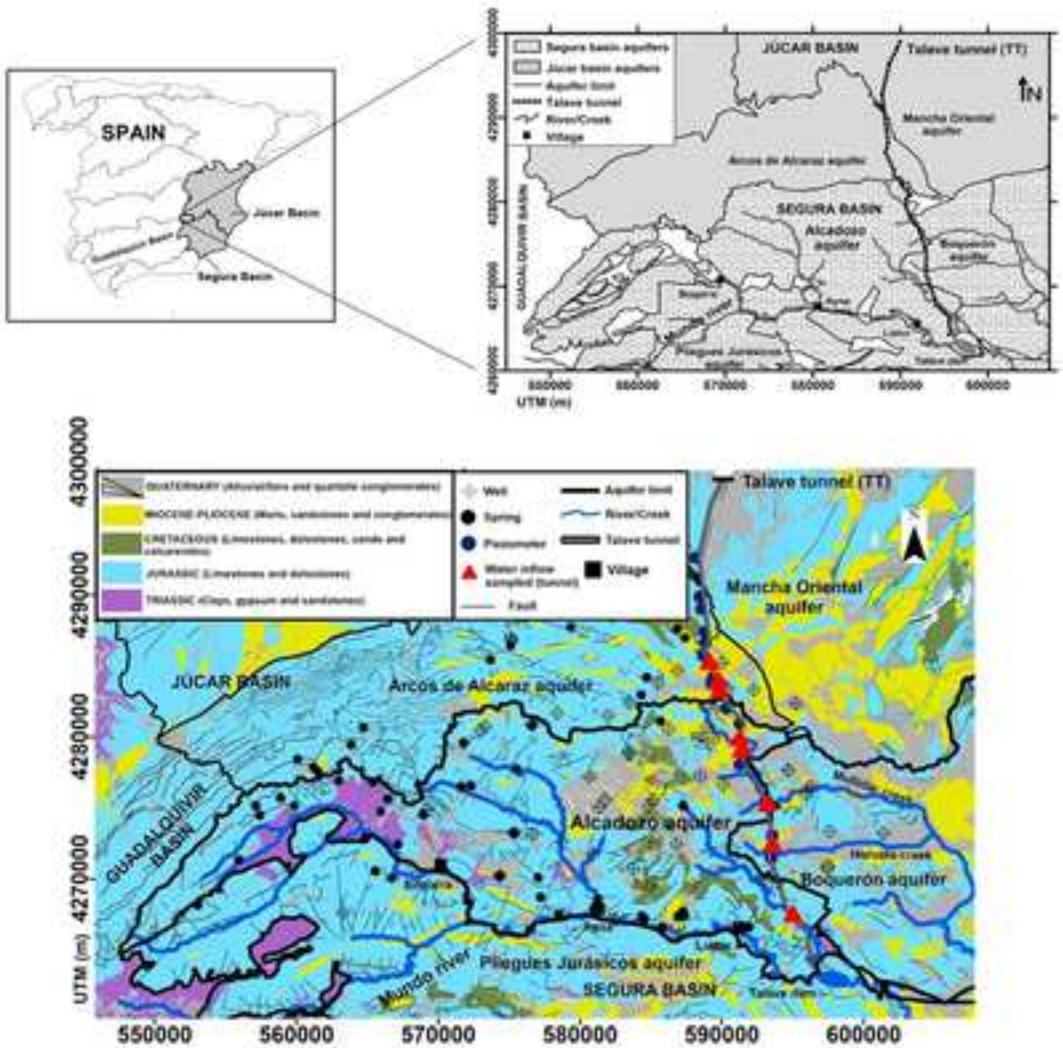

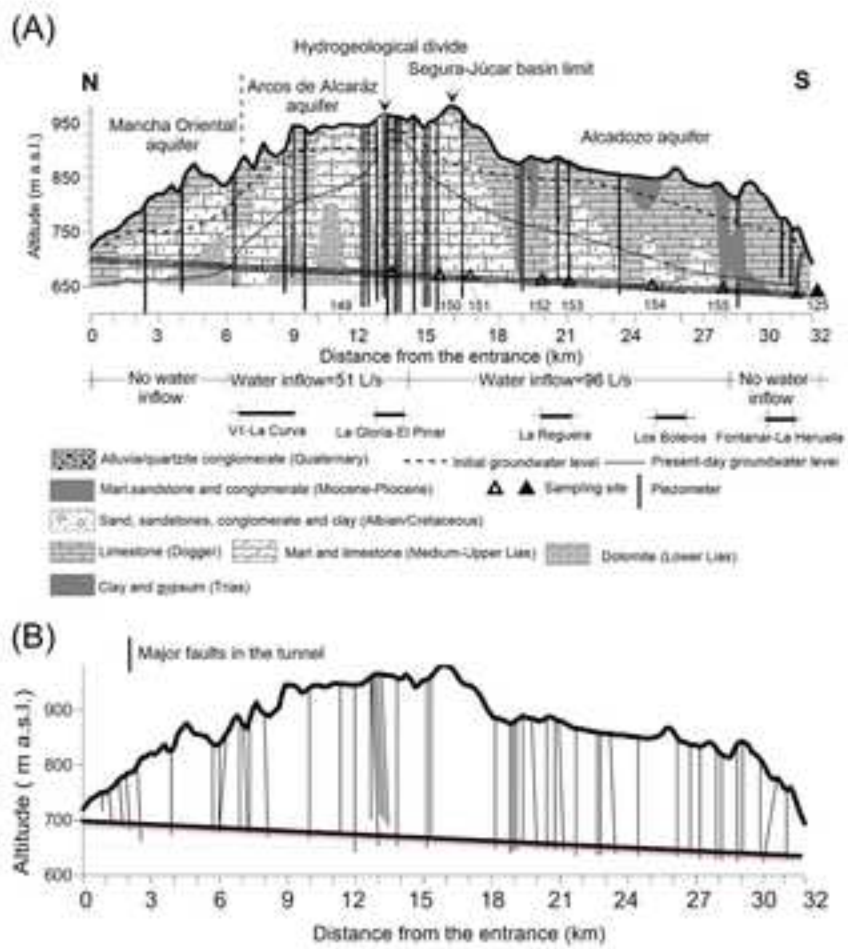
(A)
Hydrogeological divide
Segura-Júcar basin limit
N
S
Arcos de Alcaráz aquifer
Mancha Oriental aquifer
Alcadozo aquifer
Altitude (m a.s.l.)
950
850
750
650
0
3
6
9
12
15
18
21
24
27
30
32
Distance from the entrance (km)
No water inflow
Water inflow=51 L/s
Water inflow=96 L/s
No water inflow
La Reguera
Clay and gypsum (Trias)
(B)
Major faults in the tunnel
Altitude (m a.s.l.)
900
800
700
600
0
3
6
9
12
15
18
21
24
27
30
32
Distance from the entrance (km)

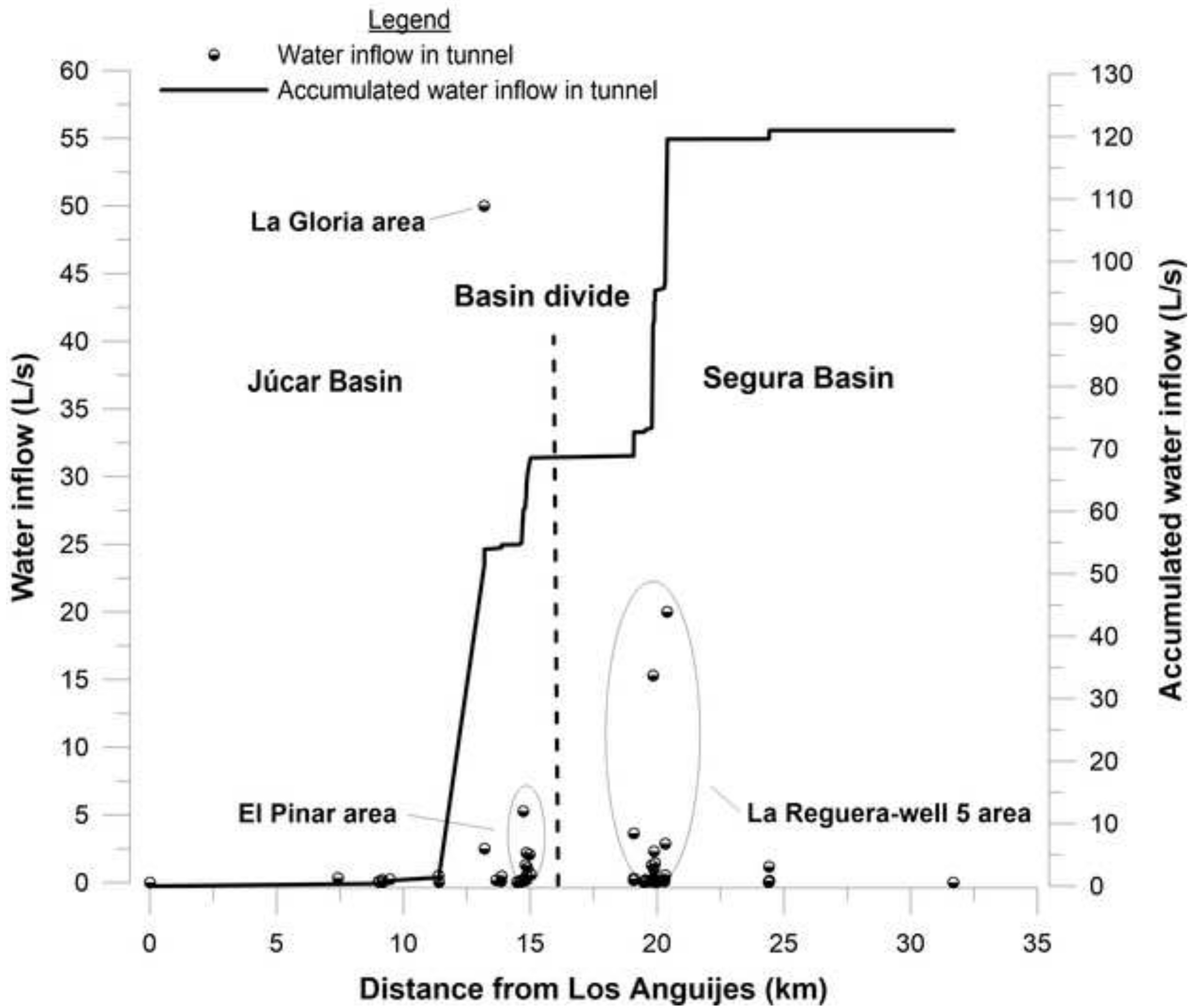
Legend
Water inflow in tunnel
Accumulated water inflow in tunnel
La Gloria area
Basin divide
Júcar Basin
Segura Basin
El Pinar area
La Reguera-well 5 area
Water inflow (L/s)
Accumulated water inflow (L/s)
Distance from Los Anguijes (km)
0
5
10
15
20
25
30
35
40
45
50
55
60
70
80
90
100
110
120
130

Figure

Click here to access/download;Figure;Figura 4.jpg

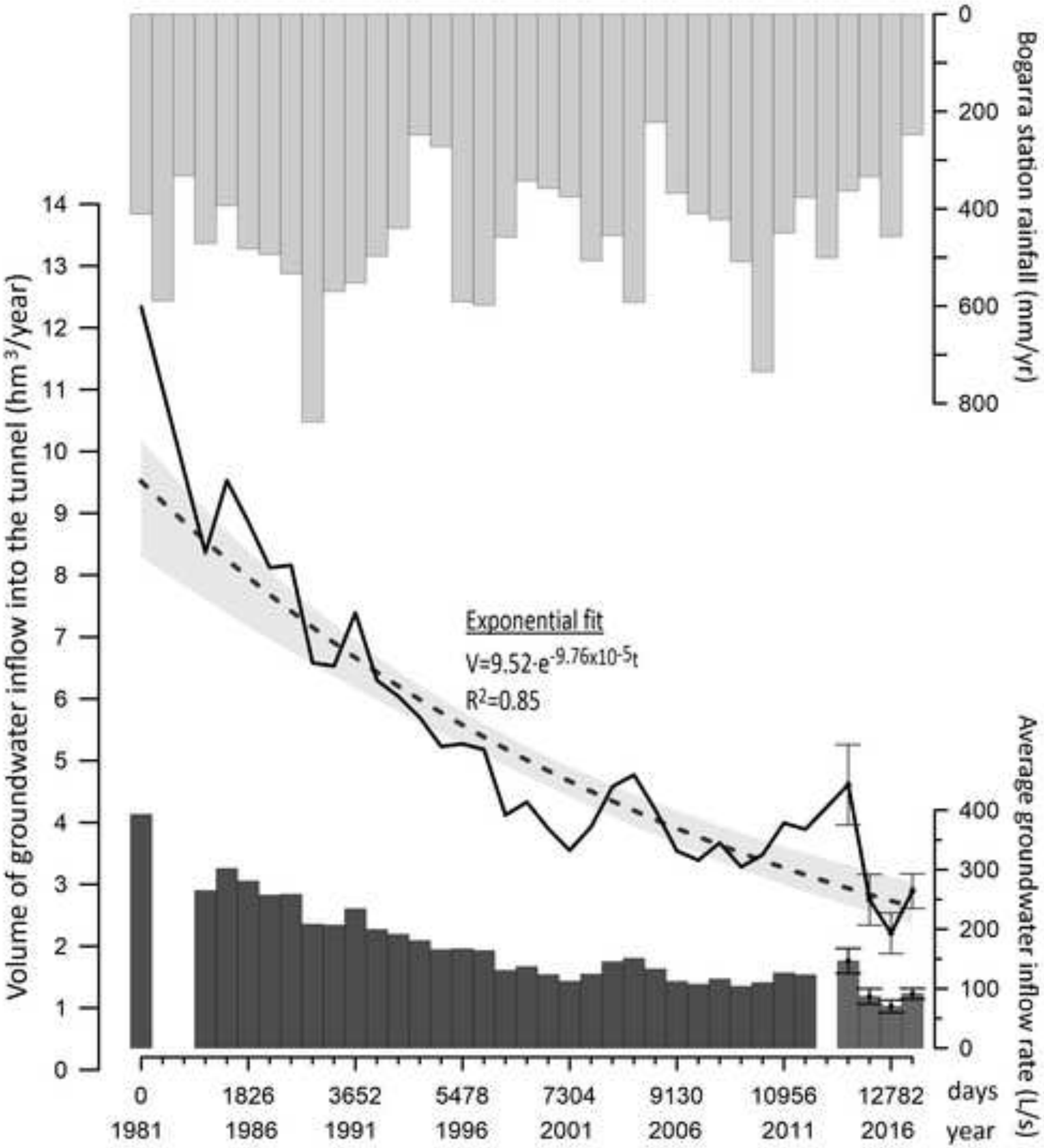

Figure Click here to access/download;Figure;Figura 5.jpg

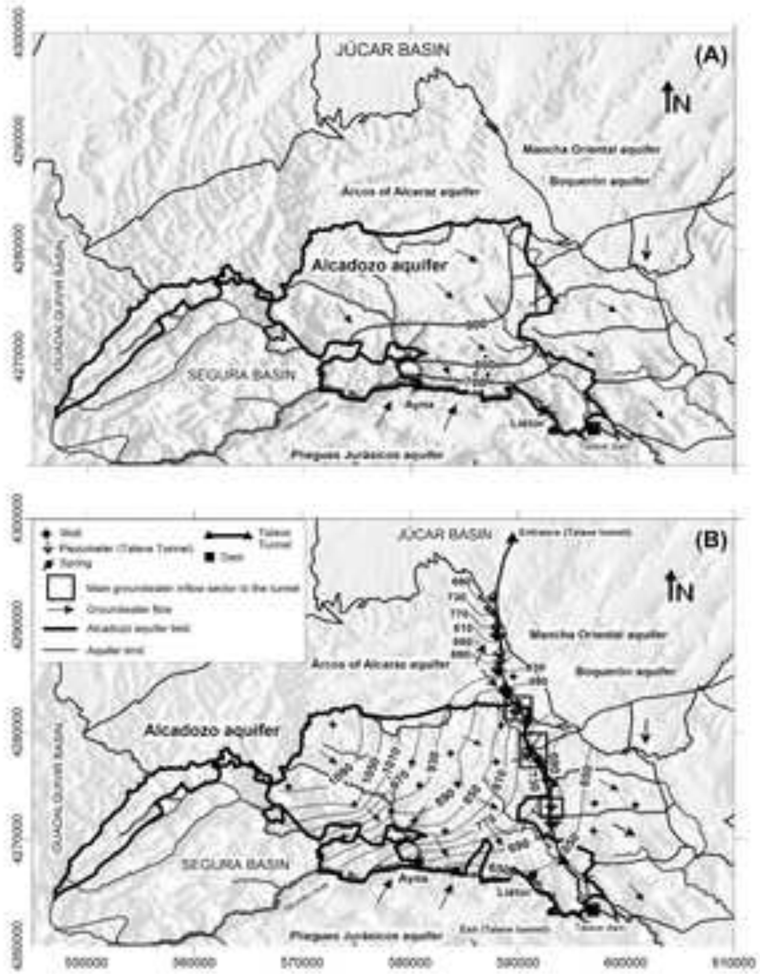

Figure

Click here to access/download;Figure;Figura 6.jpg

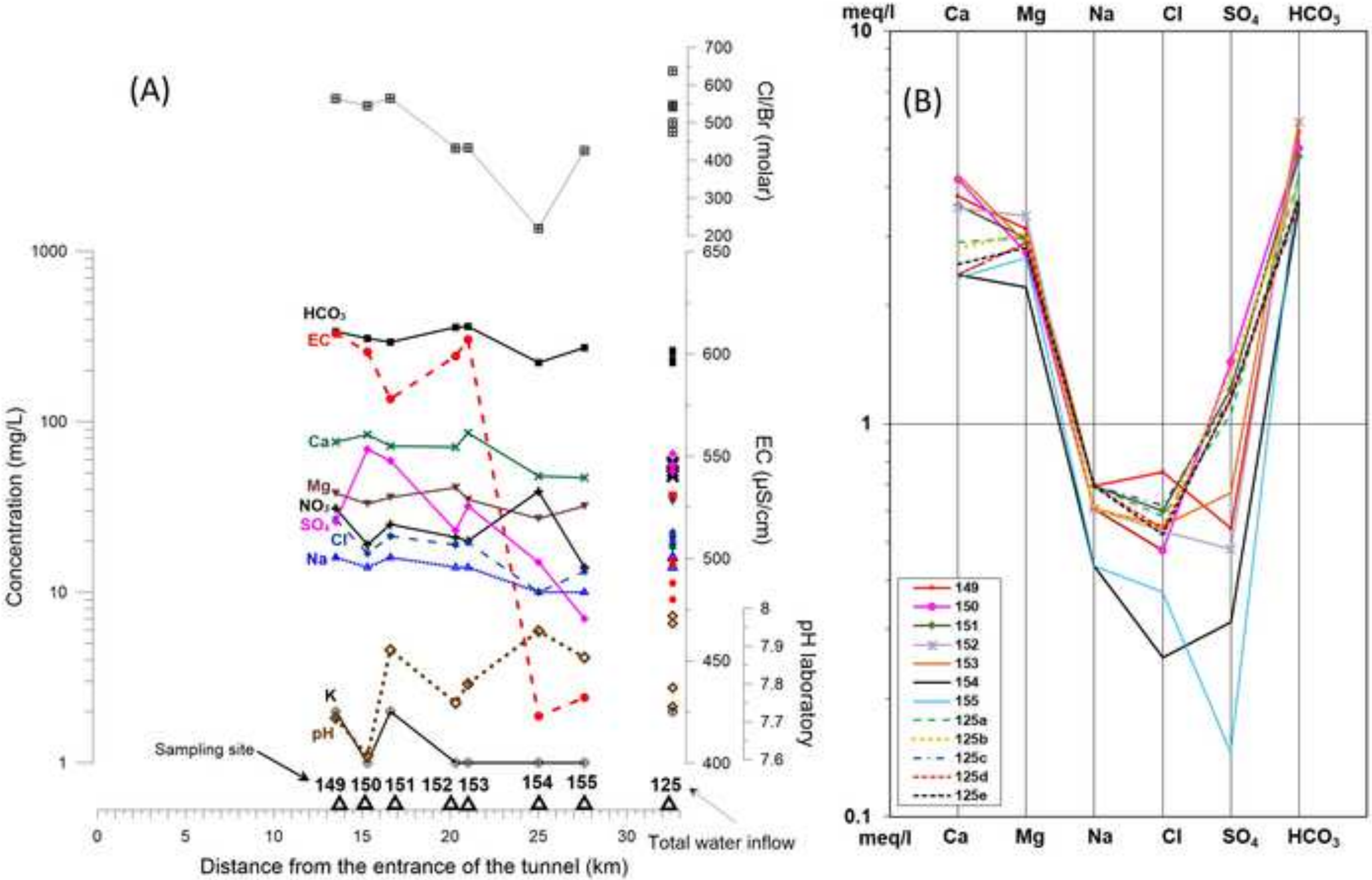

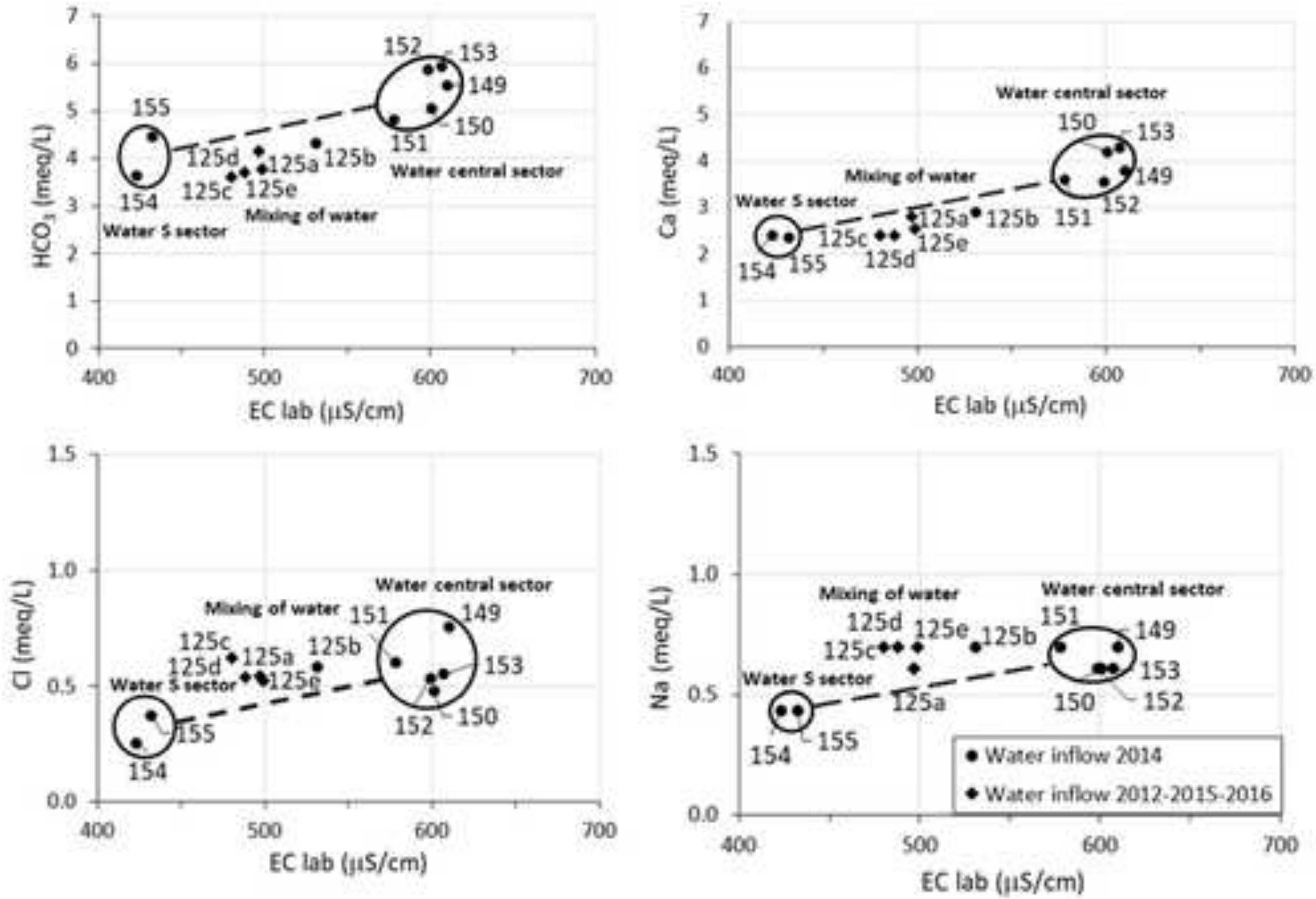

HCO3 (meq/L)
EC lab (µS/cm)
155
154
152
153
149
150
151
125d
125a
125b
125c
125e
Water central sector
Mixing of water
Water S sector
Ca (meq/L)
Cl (meq/L)
Na (meq/L)
Water inflow 2014
Water inflow 2012-2015-2016

Figure

Click here to access/download;Figure;Figura 8.jpg

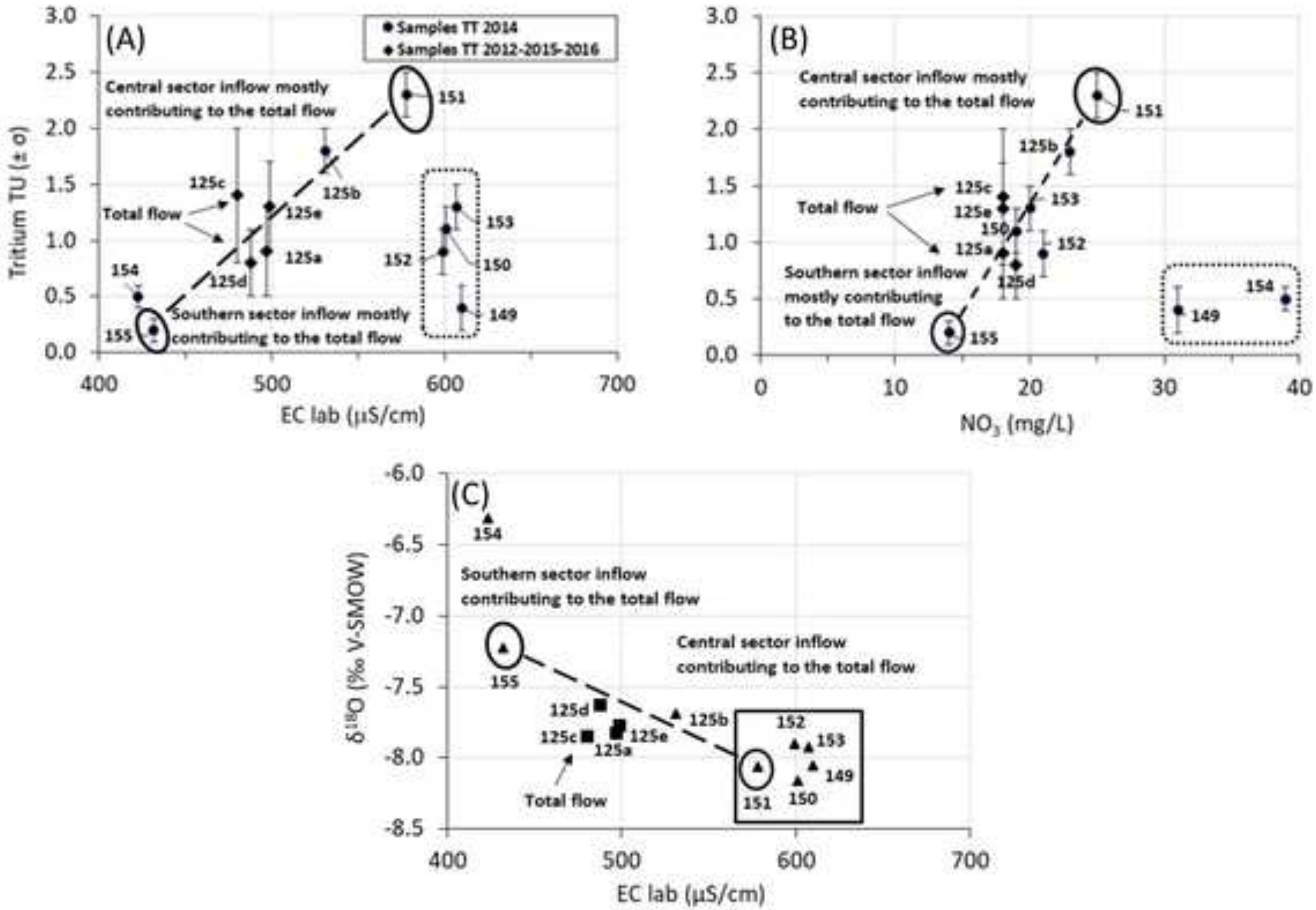

CRedit authors statement

Jorge Hornero: Conceptualization, Methodology, Formal analysis, Investigation, Writing-Original Draft; **Marisol Manzano**: Conceptualization, Methodology, Formal analysis, Writing-Original Draft; **Emilio Custodio**: Writing - Review & Editing.

Declaration of interests

☒ The authors declare that they have no known competing financial interests or personal relationships that could have appeared to influence the work reported in this paper.

☐The authors declare the following financial interests/personal relationships which may be considered as potential competing interests: